Site C Clean Energy Project

Peace River Water Level Fluctuation Monitoring Program (Mon-17)

Tasks 3a to 3e

Construction Year 3 (2017)

Brian Ma, PhD
ESSA Technologies Ltd.

Eric Parkinson, MSc
ESSA Technologies Ltd.

Michael McArthur, MSc, RPBio
BC Hydro

Dustin Ford, RPBio
Golder & Associates Inc

Sima Usvyatsov, PhD
Golder & Associates Inc

Tanya Seebacher, MSc, RPBio
Golder & Associates Inc

August 2018

Table of Contents

List of Figures:

List of Tables:

1 INTRODUCTION (LEARNING)

In accordance with Provincial Environmental Assessment Certificate Condition No. 7 and Federal Decision Statement Condition Nos. 8.4.3 and 8.4.4 for BC Hydro's Site C Clean Energy Project (the Project), BC Hydro developed the Site C Fisheries and Aquatic Habitat Monitoring and Follow-up Program (FAHMFP).

The hydrograph of the Peace River is expected to change post-Project. The Peace River Water Level Fluctuations Monitoring Program (Mon-17) represents one component of the FAHMFP and is designed to understand how changes to the daily hydrograph from Project operations could affect fish populations by altering the amount or quality of fish habitat. As stated in Mon-17, "*During Project operation, daily discharge fluctuations are expected to increase and phase shifted to different times of the day. The daily range of water levels is predicted to increase from 0.5 m to 1.0 m at the Site C tailrace, increase from 0.4 m to 0.8 m near Taylor, BC, and increase from 0.5 m to 0.9 m near the Alces River confluence.*" These changes in discharge could influence fish growth or survival (as summarized in the Environmental Impact Statement (EIS) Volume 2, Section 12).

Mon-17 is predominately analysis-focused and represents a synthesis of information collected under other FAHMFP programs. The only data collection task specific to Mon-17 is Task 2a during Construction Years 3 and 4 – small fish sampling of otoliths for three indicator species, which will be a dedicated field survey as part of this monitoring program.

During the construction phase, analysis and data collection is used to quantify baseline conditions which will be used to compare against when discharge changes during Project operation.

1.1 MANAGEMENT QUESTIONS AND HYPOTHESES:

Mon-17 poses a series of management questions and hypotheses. The management questions are –

1. How do changes in the hydrological regime affect estimates of catchability used in the Peace River Fish Community Monitoring Program (Mon-2)?
2. How do changes in the hydrological regime affect fish and fish habitat of the Peace River?

To support the management questions, the following management hypotheses, posed as a series of null hypotheses, were presented in Mon-17:

H_{1a}: Species-specific catchability at a sampling site in the Peace River is independent of the water level at the time of sampling.

H_{1b}: Species-specific catchability at a sampling site in the Peace River is independent of the pattern of variation in water level during the month prior to sampling, (The term "water level regime" to distinguish this effect from that of "water level at the time of sampling").

H_2: Periphyton production among and within sites in the Peace River is independent of the magnitude and timing of flow fluctuations.

H_3: Biomass of invertebrates (benthos) among and within sites in the Peace River is independent of the magnitude and timing of flow fluctuations.

H_4: Species-specific fish growth of age-0 and age-1 fish among sites in the Peace River is independent of the magnitude and timing of flow fluctuations.

H_5: Species-specific fish density among sites, as a measure of species composition, in the Peace River is independent of the magnitude and timing of flow fluctuations.

H_6: Species-specific recruitment is independent of the magnitude and timing of flow fluctuations.

1.2 TASKS AND SCHEDULE

The analysis tasks that are conducted in Mon-17 are shown in Table 1, which also highlights the hypotheses each task addresses and the related data collection tasks. The schedule for analysis and supporting data collection tasks for Mon-17 are shown in Table 2. For 2017 (Construction Year 3), there was a commitment to collect small fish otoliths (Mon-17, Task 2b). There was no commitment to analyze data for 2017, but BC Hydro elected to do an initial analysis of data based on the information at hand for Tasks 3a, 3c, and 3e because data were available for these three tasks.

Table 1: Peace River Water Level Fluctuation Monitoring Program (Mon-17) analysis tasks with hypotheses addressed and related data collection tasks

Analysis Task	Hypotheses addressed	Related Data Collection Tasks
Task 3a – Catchability Examine the relationship between site-specific boat electroshocking catch rates to discharge at the time of sampling	H_{1a}, H_{1b}	**Mon-2, Task 2a –** Peace River Large Fish Indexing Survey
Task 3b – Benthos and Periphyton Examine the relationship between accrual of periphyton and benthos and flow variables and habitat conditions	H_2, H_3	**Mon-7** periphyton and benthos data
Task 3c – Daily Growth Examine the relationship between the width of daily growth rings on otoliths of indicator small fish species to daily flow variations	H_4	**Mon-2, Task 2b** – Peace River Fish Composition and Abundance Survey **Mon-17, Task 2b** – "Small Fish" (Construction Years 3 and 4 only)
Task 3d – Fish Community Composition Examine the relationship between fish community composition and flow fluctuations	H_5	**Mon-2, Task 2a** – Peace River Large Fish Indexing Survey **Mon-2, Task 2b** – Peace River Fish Composition and Abundance Survey
Task 3e – Fish Recruitment Examine the relationship between population age-structure data to seasonal patterns in flow fluctuations	H_6	**Mon-2, Task 2a** – Peace River Large Fish Indexing Survey

Table 2: Schedule (for Construction Years only) for Peace River Water Level Fluctuation Monitoring Program (Mon-17) analysis tasks and related data collection tasks. The current sampling and analysis year is highlighted in red. "XX" is used to note years where tasks are performed.

	CALENDAR YEAR									
	2015		2017			2020				2024
	CONSTRUCTION YEAR									
Analysis Tasks	1	2	3	4	5	6	7	8	9	10
17: Peace River Water Levels Flucuations Monitoring Program										
Task 3a: Catchability		XX		XX						
Task 3b: Benthos and Periphyton				XX						
Task 3c: Daily Growth				XX						
Task 3d: Fish Community Composition				XX						
Task 3e: Fish Recruitment				XX						
Supporting Data Collection Tasks										
17: Peace River Water Levels Flucuations Monitoring Program										
Task 2b: Small Fish Otolith Collection			XX	XX						
2: Peace River Fish Community Monitoring Program										
Task 2a: Peace River Large Fish Indexing Survey	XX	XX	XX	XX	XX	XX	XX	XX	XX	XX
Task 2b: Peace River Fish Composition and Abundance Survey						XX	XX			XX
Task 2c: Peace River Creel Survey						XX				
Task 2d: Offset Effectiveness Monitoring Program			XX	XX	XX					
Task 2e: Peace River Tributaries Walleye Spawning and Rearing Use Survey					XX			XX		
Task 2f: Beatton River Arctic Grayling Status Assessment			XX	XX						XX
7: Peace River Fish Food Organisms Monitoring Program			XX	XX						

2 METHODS AND RESULTS BY TASK (DOING)

2.1 DISCHARGE DATA

Discharge data was gathered from Water Survey of Canada hydrometric stations for use in Mon-17 analyses. In most cases, analyses focused on Section 5 of the Peace River. Discharge data was collected in the middle of Section 5 at the Peace River above the Pine River (07FA004) hydrometric station (https://wateroffice.ec.gc.ca/search/historical_e.html). These discharge data are collected as cubic metres per second (cms).

Section 5 was selected because this section of river will experience fluctuating water levels during Project operations, and it is the only fish index study area in the Peace River mainstem that will remain riverine following construction. Furthermore, Section 5 has sufficient historical data to cover a wide range of flow levels. Section 5 is located between the Moberly River confluence to near the Canadian National Railway bridge, between river km 53.4 and 64.8, measured from the BC/AB border (Mainstream 2011). We expect that the analysis could be expanded to Sections 6, 7, and 9 as the Peace River Large Fish Indexing Survey (Mon-2, Task 2a) continues to collect data.

The historical and predicted flows from this station demonstrate a wide range of flow conditions (Table 3), although the predicted flows during Project operations are expected to have a larger range. The post-Project estimated median flow for the sampling time of day and time of year is similar to historic (2000-2015) levels (1,151 vs. 1,231cms; Table 1), and the 90th and 10th percentile flows post project (390 and 1,780 cms) shows a wider range of conditions than seen in the 2000-2015 sampling period (485 and 1,640 cms).

Table 3: Historical and predicted flows for the August-September period at the Water Survey of Canada Peace River above Pine River hydrometric station.

	All Day Exceedances			Daylight Sampling Hours (08:00 - 17:00 local time) Exceedances			Non-sampling hours (0:00 - 7:00; 18:00 - 23:00, local time) Exceedances		
Period	10%	50%	90%	10%	50%	90%	10%	50%	90%
Historical Data (1979 - 1999)*	1651	1073	442	1574	977	436	1703	1152	450
Historical Data (2000 - 2009, 2010, 2014 - 2015)	1592	908	442	1724	1240	449	1467	855	441
Predicted Site C Flows* & **	1714	995	390	1780	1231	390	1540	746	390

* Based on the years 1979 through 1999 excluding 1980, 1981, 1983 and 1987 due to a lack of data in August and September (less than 50% data available)
** Predicted flows were completed using BC Hydro's GOM modeling, more information on this modeling is contained in the surface water section of the EIS.

2.2 CATCHABILITY (TASK 3A)

2.2.1 Introduction

Changes in the hydrograph, along with other changes to habitat conditions at the time of sampling, can lead to changes in electrofishing sampling efficiency or catchability (*q*) (Speas et al. 2004, Lyon et al. 2014). If a relationship exists between flow conditions and catchability for fish in the Peace River, this might affect the interpretation of the Mon-2, Task 2a results such as species abundance comparisons before and during the operation of the Project. Ultimately, catchability (and catch per unit effort (CPUE)) will be used as proxies for abundance of large

fish species, and therefore, it is necessary to be able to disentangle any potential effects of discharge in determining changes.

This analysis was proposed to understand whether species-specific catchability would be dependent on flow fluctuations. Task 3a will test Hypotheses 1a and 1b:

H_{1a}: Species-specific catchability at a sampling site in the Peace River is independent of the water level at the time of sampling.

H_{1b}: Species-specific catchability at a sampling site in the Peace River is independent of the pattern of variation in water level during the month prior to sampling, (The term "water level regime" to distinguish this effect from that of "water level at the time of sampling").

A previous preliminary effort to examine the relationship between CPUE and discharge demonstrated no effect of discharge on the day of sampling compared to CPUE for Mountain Whitefish in Section 5 of the Peace River. This preliminary analysis is included as Appendix A.

2.2.2 Methods

To test Hypotheses 1a and 1b, we examined the relationship between species-specific CPUE data with changes in flow in the Peace River for Mountain Whitefish, Bull Trout, and Arctic Grayling using a series of general linear models. CPUE is related to catchability following equation 1:

$$CPUE = qN \qquad \text{(equation 1)}$$

where the population (N) is defined as the abundance of fish of a given species within a reach, and q is defined as the proportion of the population captured by a unit of sampling effort (i.e., catchability). By measuring *CPUE*, we can understand how changes in habitat conditions, such as discharge, can affect catchability (q). Potential mechanisms can involve the capture process and/or fish behaviour and can vary among locations and species. For example, q could be lower if fish move to higher depth/velocity habitat or if correlated factors affect the behaviour or visibility of target fish (e.g., turbidity, temperature).

We focused our analysis on Hypothesis 1a, focusing on the species and space with the largest possible change in catchability (i.e., largest effect size) due to changes in flow from Project operations.

CPUE data was calculated from large fish indexing data collected during the pre-Project phase (Peace River Fish Community Indexing Program, GMSMON-2, from 2004 to 2014) and under Mon-2 in Construction Years 1 to 3 (2015 to 2017). Each data point represents the average CPUE for a unique sample date. We chose to focus our analysis on Mountain Whitefish in Section 5. Because Mountain Whitefish in Section 5 are the most numerically abundant of the large fish species, the effects of sub-sampling error are expected to be much less than the other target species, Arctic Grayling and Bull Trout, and therefore, most likely to show a change in CPUE.

To align the sampling frame between CPUE and flow data, we only used discharge data during periods most representative of conditions for large fish index sampling (Mon-2, Task 2a). This was typically during the mid-August to early October months. For sampling years 2000 to 2015, the average discharge on the day of sampling, for working hours (08:00-17:00hrs local time), was compared to CPUE collected on the same day (although other time lags could be explored for Hypothesis 1b).

We used a series of linear regression models to explore the relationship between CPUE and discharge while accounting for a sampling year effect. We used an information theoretic approach to select the best model amongst the competing models – Akaike Information Criterion (AIC). To ensure the same data set was used to compare models, we only used data where both CPUE and discharge data were available on the same day. In the raw data, there were some days where the discharge data were not available.

CPUE was analyzed as both catch per second (#/s) and catch per 100 m (#/100 m). We explore the relationship with CPUE to a linear relationship with discharge (D). We also considered different functional forms to account for a Year effect. The general form of the model is shown in equation 2:

$$CPUE_{ij} \sim D_{ij} + f(Y_i) \qquad \text{(equation 2)}$$

where $CPUE_{ij}$ is the CPUE in sample year i in sampling bout j. Discharge for each sample year and sampling bout combination is represented as D_{ij}. The different functional forms of the year effect is represented with the general function $f(Y_i)$. To normalize the CPUE data, we used a log-transformation of CPUE + ½ minimum non-zero CPUE value. This is a widely-accepted rule-of-thumb transformation for CPUE data.

The discharge data used was from the day of sampling. The linear discharge function is shown in equation 3:

$$f(D_{ij}) = a + bD_{ij} \qquad \text{(equation 3)}$$

where a and b are the intercept and slope of the linear regression model.

Changes in CPUE from a year effect might be linked to changes in abundance from year-to-year. CPUE is related to catchability *and* abundance (eq. 1), so a year-to-year change in CPUE might be caused by changes in abundance rather than catchability from year-to-year. These changes in CPUE and abundance might be from random deviation away from a mean abundance (N) each year (i), or from a trend in abundance away from a mean.

The first functional form of the year effect is to treat each year as an independent event (i.e., year as a factor). This functional form is consistent with changes in abundance from year-to-year natural variability (i.e., process error) (equation 4):

$$f(Y_i) = Y_i \qquad \text{(equation 4)}$$

We also considered the year effect as linear (equation 5) and quadratic functions (equation 6), where c_1, c_2, and c_3 are parameters for the linear and quadratic functions. These functional forms are consistent with a true pattern in abundance from year-to-year.

$$f(Y_i) = c_1 + c_2 Y_i \qquad \text{(equation 5)}$$

$$f(Y_i) = c_1 + c_2 Y_i + c_3 Y_i^2 \qquad \text{(equation 6)}$$

We combined the discharge and different functional forms of the year effect into a series of models, as shown in Table 4. These models were run for Mountain Whitefish, Bull Trout, and Arctic Grayling (and for the different measurements of CPUE). Model fitting using the linear model function in R (lm()) was used to minimize the sum of squares of observed and predicted $CPUE_{ij}$ values for the different functional forms of the model. The best models were selected

based on the AIC values of the models. Models that had a ΔAIC of <2 from the best model are thought to be as good at describing the relationship (Burnham and Anderson, 2002).

Table 4: Models compared in the model selection approach to determine if there is a relationship between CPUE and daily discharge. All models are analyzed using both catch-per-unit-time and catch-per-unit-length for Mountain Whitefish, Bull Trout, and Arctic Grayling.

Model Number	Description
1	CPUE does not vary with discharge or year
2	Discharge effect
3	Year *i* effect (factor)
4	Linear Year effect
5	Quadratic Year effect
6	Discharge effect and Year *i* effect
7	Discharge effect and Linear Year effect
8	Discharge effect and Quadratic Year effect

2.2.3 Results

1. Mountain Whitefish

Changes in CPUE, as measured by catch-per-unit-time (#/s) and catch-per-unit-length (#/100 m), for Mountain Whitefish in Section 5 of the Peace River are best described by a model that only accounts for a curvilinear sample year effect and does not account for discharge (Model 5) (CPUE (#/s) – Table 5; CPUE (#/100 m) – Table 6). These results indicate that there may be an underlying trend in the year-to-year change in CPUE that follows a curvilinear function, peaking in 2009 to 2011 and declines in recent years. The best fit models are shown in Figure 1. However, for both measures of CPUE, there is little evidence that this model is different from one that describes a random year effect (Model 3) or one that includes a curvilinear year effect and a discharge effect (Model 8).

A closer look at the model fit, based on the output of the linear model, shows that the adjusted R^2 values for the three models are similar (#/s – Table 5; #/100 m – Table 6), and that generally, the best fit model explained a higher proportion of the variability in CPUE as measured in catch-per-unit-time (adjusted R^2 = 0.645) than CPUE as measured in catch-per-unit-length (adjusted R^2 = 0.479). For both measures of CPUE, while the AIC was similar to the model that included a discharge effect (Model 8), this discharge term was not significant (CPUE (#/s) – P = 0.316; CPUE (#/100 m) – P = 0.719). If we adopted a frequentist approach to model selection (rather than the information theoretic approach we chose to use), discharge would not be included as an explanatory variable. Model outputs are shown in Appendix B.

Overall, the findings suggest that there is a significant effect of the sample year on the data, and that there is a curvilinear trend in the data with a recent decline in Mountain Whitefish abundance. Furthermore, there is limited evidence of an effect of discharge on CPUE of Mountain Whitefish in Section 5, but the effect of this parameter is not statistically significant.

Table 5: Results from statistical models considered to explain changes in Mountain Whitefish CPUE (#/s) in Section 5 of the Peace River as a function of sample year and discharge. The lowest AIC value indicates the best model, which is denoted using ''. Other models that belong to the family of best fit models are denoted using '*'. Adjusted R^2 values and degrees of freedom are also shown.**

Model	df	Adjusted R^2	AIC	ΔAIC
5**	127	0.645	33.96	0.00
3*	117	0.668	34.29	0.33
8*	126	0.645	34.91	0.96
6	116	0.666	36.19	2.23
4	128	0.370	107.39	73.44
7	127	0.366	109.14	75.19
2	128	0.022	164.54	130.59
1	129	0.000	166.44	132.49

Table 6: Results from statistical models considered to explain changes in Mountain Whitefish CPUE (#/100 m) in Section 5 of the Peace River as a function of sample year and discharge. The lowest AIC value indicates the best model, which is denoted using ''. Other models that belong to the family of best fit models are denoted using '*'. Adjusted R^2 values and degrees of freedom are also shown.**

Model	df	Adjusted R^2	AIC	ΔAIC
5**	127	0.479	12.74	0.00
3*	117	0.510	14.20	1.46
6*	116	0.513	14.20	1.46
8	126	0.475	14.66	1.93
4	128	0.260	57.46	44.72
7	127	0.263	57.87	45.13
2	128	0.036	91.76	79.02
1	129	0.000	95.53	82.80

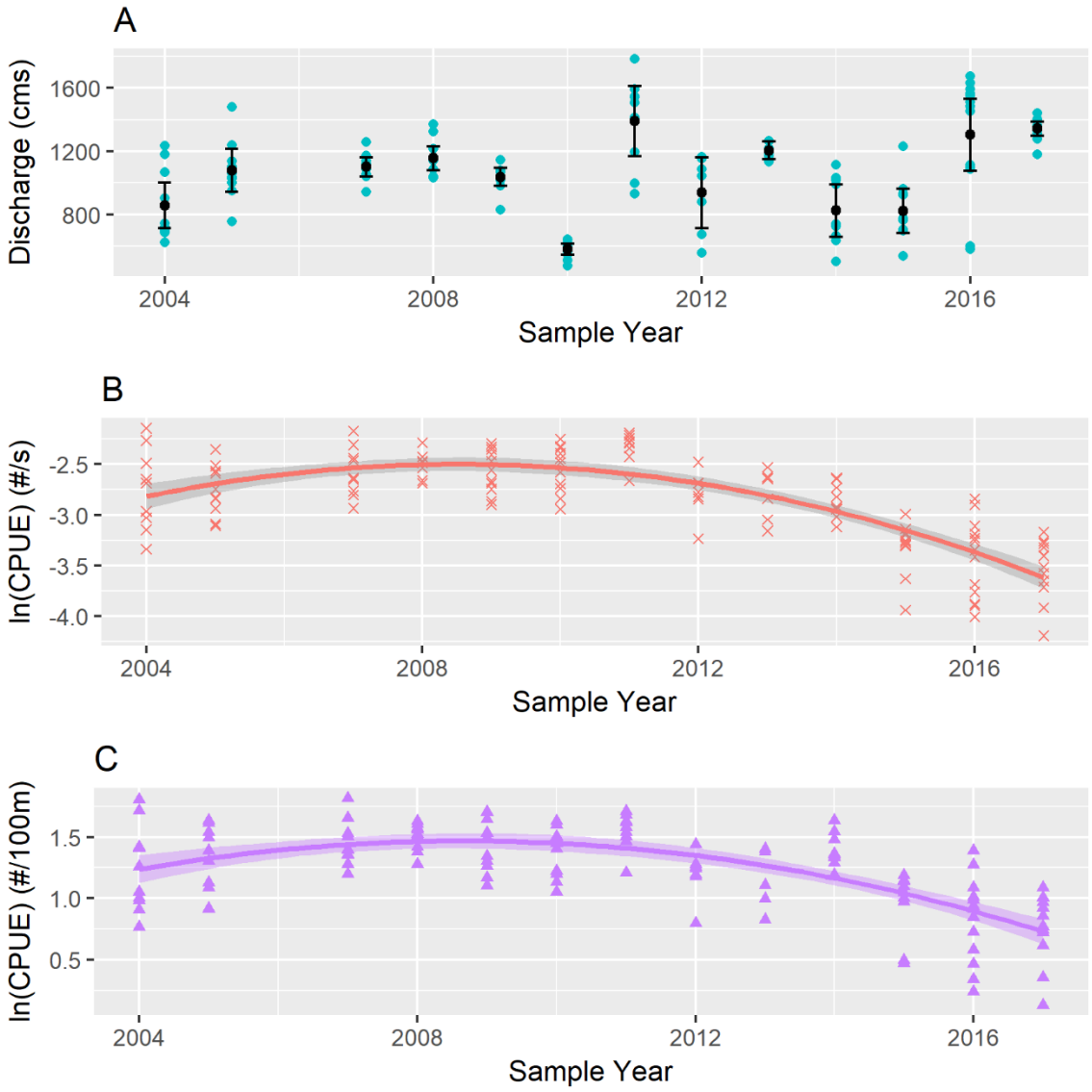

Figure 1: Mountain Whitefish CPUE, measured in catch-per-unit-time (#/s) and catch-per-unit-length (#/100 m) in Section 5 of the Peace River as a function of sample year and discharge. Panel A shows the discharge in each sample year in cms; Panel B shows the best model for CPUE (#/s) as a function of sample year; Panel C shows the best model for CPUE (#/100 m) as a function of sample year. CPUE transformation follows a log(CPUE + ½ minimum non-zero CPUE). The error bars represent the 95% confidence intervals. Discharge is not included in the best model.

2. Bull Trout

Changes in CPUE as measured in catch-per-unit-time (#/s) and catch-per-unit-length (#/100 m) for Bull Trout in Section 5 of the Peace River are best described by a model that accounts for a random sample year effect but no discharge effect (Model 3) (CPUE (#/s) – Table 7; CPUE (#/100 m) - Table 8). This model suggests there is no underlying trend in changes in CPUE from year-to-year. The best fit models are shown in Figure 2. However, there is no evidence that this model is different from one that includes a discharge effect (Model 6) based on the rule-of-thumb threshold of a ΔAIC of <2 (Burnham and Anderson, 2002). A closer look at the model fit, based on the output of the linear model, shows that while the AIC is similar for the two models, the discharge effect is not significant in Model 6 (CPUE (#/s) – P=0.299; CPUE (#/100 m) – P=0.618). If we adopted a frequentist approach to model selection (rather than the information theoretic approach), discharge would not be included as an explanatory variable. Model outputs are shown in Appendix B.

Overall, the findings suggest that there is a significant effect of the sample year on the data, but that this effect does not follow a trend. Furthermore, there is some evidence of an effect of discharge on CPUE of Bull Trout in Section 5, but the effect of this parameter is not statistically significant.

Table 7: Results from statistical models considered to explain changes in Bull Trout CPUE (#/s) in Section 5 of the Peace River as a function of sample year and discharge. The lowest AIC value indicates the best model, which is denoted using ''. Adjusted R^2 values and degrees of freedom are also shown.**

Model	df	Adjusted R^2	AIC	ΔAIC
3**	111	0.284	172.81	0.00
6*	110	0.285	173.59	0.78
8	120	0.176	181.94	9.13
2	122	0.162	182.02	9.21
7	121	0.155	184.02	11.21
1	123	0.000	202.96	30.14
4	122	0.000	203.89	31.08
5	121	0.005	204.34	31.53

Table 8: Results from statistical models considered to explain changes in Bull Trout CPUE (#/100 m) in Section 5 of the Peace River as a function of sample year and discharge. The lowest AIC value indicates the best model, which is denoted using ''. Adjusted R^2 values and degrees of freedom are also shown.**

Model	df	Adjusted R^2	AIC	ΔAIC
3**	111	0.313	158.32	0.00
6*	110	0.308	160.04	1.72
7	121	0.183	170.41	12.09
8	120	0.177	172.28	13.96
2	122	0.159	172.99	14.67
4	122	0.061	186.76	28.44
5	121	0.053	188.72	30.40
1	123	0.000	193.54	35.22

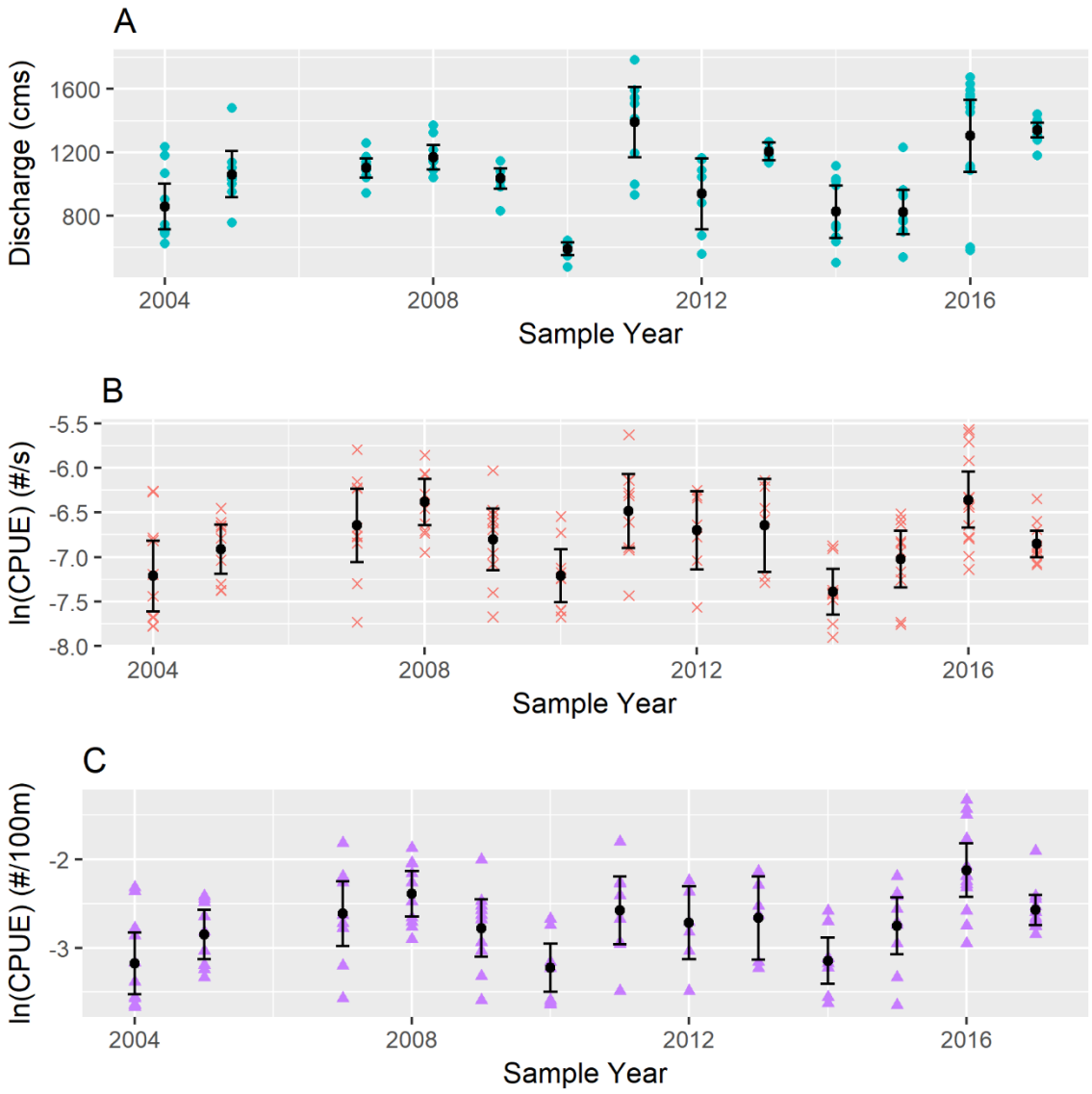

Figure 2: Bull Trout CPUE, measured in catch-per-unit-time (#/s) and catch-per-unit-length (#/100 m) in Section 5 of the Peace River as a function of sample year and discharge. Panel A shows the discharge in each sample year in cms; Panel B shows the best model for CPUE (#/s) as a function of sample year; Panel C shows the best model for CPUE (#/100 m) as a function of sample year. CPUE transformation follows a log(CPUE + ½ minimum non-zero CPUE). The error bars represent the 95% confidence intervals. Discharge is not included in the best model.

3. Arctic Grayling

CPUE as measured in catch-per-unit-time (#/s) and in catch-per-unit-length (#/100 m) for Arctic Grayling in Section 5 of the Peace River lead to two different models. The best fit models are shown in Figure 3.

The best model that described changes in CPUE measured in catch-per-unit-time (#/s) was Model 7, which has a linear sample year effect and a discharge effect (Table 9). However, there is little evidence that this model is different from Model 3, which has no discharge effect and treats sample year as a factor, or from Model 8, which has a curvilinear sample year effect and a discharge effect (ΔAIC of <2). In Model 7, the discharge term was statistically significant ($P < 0.001$) and had a positive correlation with CPUE. Model outputs are shown in Appendix B.

The best model that described changes in CPUE measured in catch-per-unit-length (#/100 m) was Model 3, which has no discharge effect and treats sample year as a factor (Table 10). However, this model was not different from Model 6, which includes discharge as an effect (ΔAIC of <2). A closer comparison of the models shows that the discharge effect in Model 6 is not significant ($P = 0.357$). If we adopted a frequentist approach to model selection (rather than the information theoretic approach we chose to use), discharge would not be included as an explanatory variable. Model outputs are shown in Appendix B.

For both measures of CPUE, the proportion of variance that was explained by the best models was relatively high (CPUE (#/s) adjusted $R^2 = 0.549$; CPUE (#/100 m) adjusted $R^2 = 0.539$).

Overall, the results from our analysis on the effect of discharge and sample year on Arctic Grayling CPUE is difficult to interpret. While CPUE measured in catch-per-unit-time suggests that there is a linear decline in Arctic Grayling CPUE across years and discharge is a significant factor, CPUE measured in catch-per-unit-length suggests no discharge effect and no trend in sample year. In both models, the effect of sample year was significant. Based on the AIC values for all models considered for both measures of CPUE, we suggest that Model 3 (sample year as a factor + no discharge effect) is the best model to explain changes in CPUE for Arctic Grayling. While the AIC values for Model 7 were marginally smaller for CPUE measured in catch-per-unit-time, there was no evidence that it was a better model than Model 3. Further evidence for Model 3 being favourable over Model 7 is the higher adjusted R^2 value (Model 3 adj R^2=0.576; Model 7 adj R^2=0.549). In other words, the most parsimonious answer is that CPUE for Arctic Grayling is best explained by a random sample year effect and no discharge effect.

Table 9: Results from statistical models considered to explain changes in Arctic Grayling CPUE (#/s) in Section 5 of the Peace River as a function of sample year and discharge. The lowest AIC value indicates the best model, which is denoted using ''. Models that have a similar fit are denoted using '*'. Adjusted R^2 values and degrees of freedom are also shown.**

Model	df	Adjusted R^2	AIC	ΔAIC
7**	115	0.549	231.95	0
3*	105	0.576	233.76	1.81
8*	114	0.545	233.93	1.98
6	104	0.577	234.31	2.36
4	116	0.456	253.04	21.08
5	115	0.453	254.57	22.61
1	117	0	323.83	91.88
2	116	-0.001	324.89	92.93

Table 10: Results from statistical models considered to explain changes in Arctic Grayling CPUE (#/100 m) in Section 5 of the Peace River as a function of sample year and discharge. The lowest AIC value indicates the best model, which is denoted using ''. Models that have a similar fit are denoted using '*'. Adjusted R^2 values and degrees of freedom are also shown.**

Model	df	Adjusted R^2	AIC	ΔAIC
3**	105	0.539	226.15	0.00
6*	104	0.538	227.19	1.03
7	115	0.489	228.96	2.80
8	114	0.489	229.89	3.74
5	115	0.400	247.97	21.81
4	116	0.390	248.94	22.78
1	117	0.000	306.19	80.03
2	116	0.005	306.61	80.46

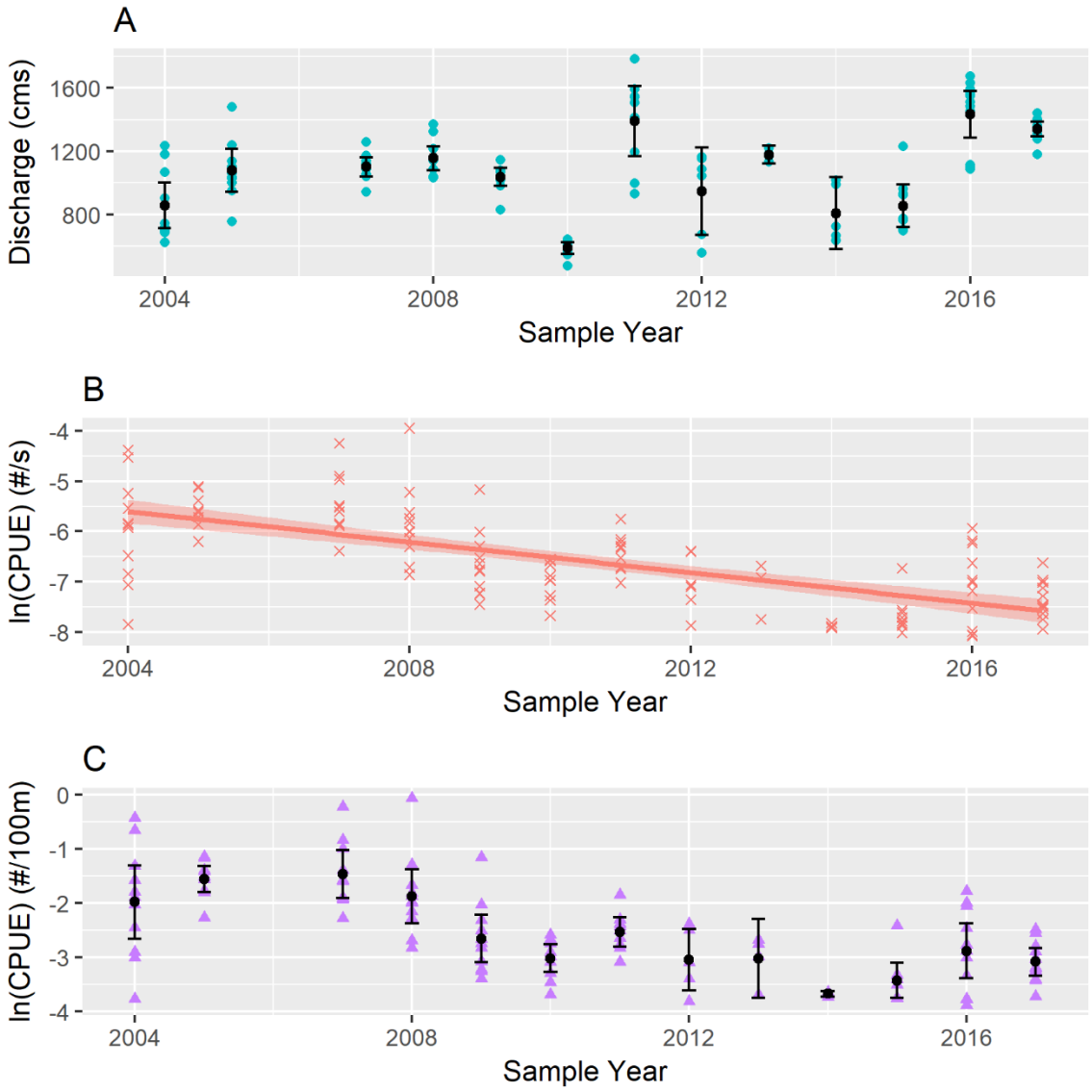

Figure 3: Arctic Grayling CPUE, measured in catch-per-unit-time (#/s) and catch-per-unit-length (#/100 m) in Section 5 of the Peace River as a function of sample year and discharge. Panel A shows the discharge in each sample year in cms; Panel B shows the best model for CPUE (#/s) as a function of sample year; Panel C shows the best model for CPUE (#/100 m) as a function of sample year. CPUE transformation follows a log(CPUE + ½ minimum non-zero CPUE). The error bars represent the 95% confidence intervals. Discharge is not included in the best model.

2.2.4 Discussion

The current analysis suggests that CPUE is not correlated with discharge on the day of sampling for all three species examined in Section 5, using data from 2004 to 2017. Instead, most of the variability in CPUE is explained by a sample year effect. For Mountain Whitefish, a curvilinear trend in CPUE was detected from year-to-year changes. For Bull Trout and Arctic Grayling, models that included sample year as a factor with no discharge effect were the best if not equally as good as other models in explaining changes in CPUE. While discharge was sometimes included in the models that were equally viable (ΔAIC of <2), the discharge effect was not statistically significant. We also note that the model that consistently shows up across all species and both measures of CPUE is Model 3, which treats sample year as a factor and has not discharge effect.

Ultimately, CPUE is a useful measure of changes in abundance if changes in catchability can be accounted for (equation 1). The results of this analysis suggest that discharge will not affect catchability, and therefore changes in CPUE can be used to track abundance. For Mountain Whitefish, a curvilinear trend in the Mountain Whitefish CPUE was observed that peaks in 2009 to 2011 and declines in recent years (Figure 1). This outcome suggests an underlying decline in abundance of Mountain Whitefish and warrants further exploration. In contrast, the abundance estimates indicate that 2010 was anomalous, particularly with respect to Section 5, which is 2-fold higher than the 2009 abundance estimate and 60% higher than the 2011 abundance estimate (bottom panel, Figure 4). At this point, it is difficult to explain these discrepancies. Abundance in Sections 1 and 3 were also highest in 2010, but the anomaly is not as great as Section 5 (bottom panel, Figure 4). Age structure analysis suggests that the 2008 cohort, which would be age-2 in 2010, was unusually strong (bottom panel, Figure 4), but this cohort should contribute strongly to catches over the next 4 to 5 years.

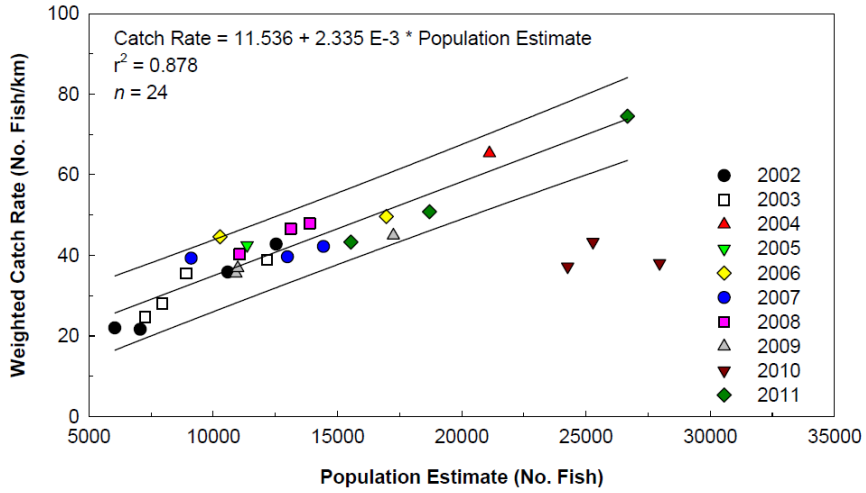

Figure 5.2.23 Relationship between population estimate and catch rate weighted for habitat of mountain whitefish during the Peace River Fish Index Project, 2002 to 2011 (data from 2010 excluded from regression; dashed lines represent 95% prediction intervals (from Mainstream and Gazey 2012).

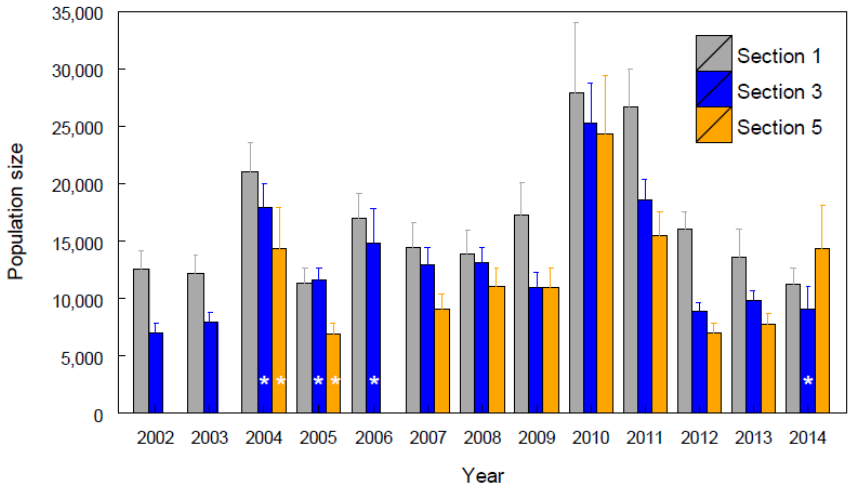

Figure 27: Population estimates with 95% confidence intervals using a Bayes sequence model for Mountain Whitefish in sample sections of the Peace River, 2002-2014. Stars denote suspect estimates due to assumption violations.

Figure 4: Top Panel: Reproduced from Mainstream 2012 of the Site C EIS. Bottom Panel: Reproduced from Golder and Gazey 2015.

2.3 BENTHOS AND PERIPHYTON (TASK 3B)

There were no planned activities to support the evaluation of the effect of flow fluctuations on benthos and periphyton as part of Mon-17 in 2017. Analysis of benthos and periphyton data will occur in Construction Year 4 (2018), with results reported in early 2019. In 2017, fish stomach content data were collected under Mon-7 using benthic basket samplers. Task 3b will test Hypotheses 2 and 3:

H_2: Periphyton production among and within sites in the Peace River is independent of the magnitude and timing of flow fluctuations.

H_3: Biomass of invertebrates (benthos) among and within sites in the Peace River is independent of the magnitude and timing of flow fluctuations.

2.4 DAILY GROWTH (TASK 3C)

2.4.1 Introduction

Otolith increment data were compared with discharge data to test Hypothesis 4:

H_4: Species-specific fish growth of age-0 and age-1 fish among sites in the Peace River is independent of the magnitude and timing of flow fluctuations.

This section provides an overall summary of the findings from the otolith study, but Appendix B should be referred to for the full analysis.

2.4.2 Methods:

Preliminary sample collection and analysis were completed in 2016 and 2017. Appendix B provides a summary of the complete results. Laboratory processing of the otoliths proved challenging because of the emphasis placed on a long series of growth rings that included the outermost ring. Earlier sampling (to avoid very narrow outer rings) and incorporation of data from otoliths with fewer rings that may not include the outer ring should improve the acceptance rate.

2.4.3 Results:

Of the 89 otoliths collected from five species in November 2016, useable data were obtained from 34 fish (all age-0 Mountain Whitefish). In addition, three age-1 Mountain Whitefish from 2014 also provided usable data. The number of daily growth rings counted and measured ranged from 24 to 56. Growth increments ranged from 4.8 to 62.4 nm, with a resolution of 2.4 nm. Average daily increments for individual fish ranged from 14 to 36 nm.

The results suggest that temperature-adjusted growth in Mountain Whitefish fry was affected by the flow experienced by the fry over the same period (Appendix A). Whether this result can be expanded to other cohorts or species is unknown. However, for this one single cohort of Mountain Whitefish fry, the null hypothesis H_4 was rejected.

Both periods of interest had strong contrasts in daily discharge variation but, in 2016, there was a coincident decline in temperature that covered most of the time period over which daily growth rings were measured (Figure 5). The range of daily discharge increased from a low of 200 cms in the first week to 900 cms over the 56-day period (black dotted line, Figure 5). Lower temperatures and higher discharges are both expected to be associated with slower growth but there is substantial short-term (~10 day) contrast in discharge variation that can be used to isolate the effect of discharge variation. The statistical model with the best AIC included additive effects of temperature (positive effect) and discharge variation (negative effect) for age-0 Mountain Whitefish and a single Longnose Sucker. In contrast, the effect of discharge variation was positive for the three age-1 Mountain Whitefish from 2014.

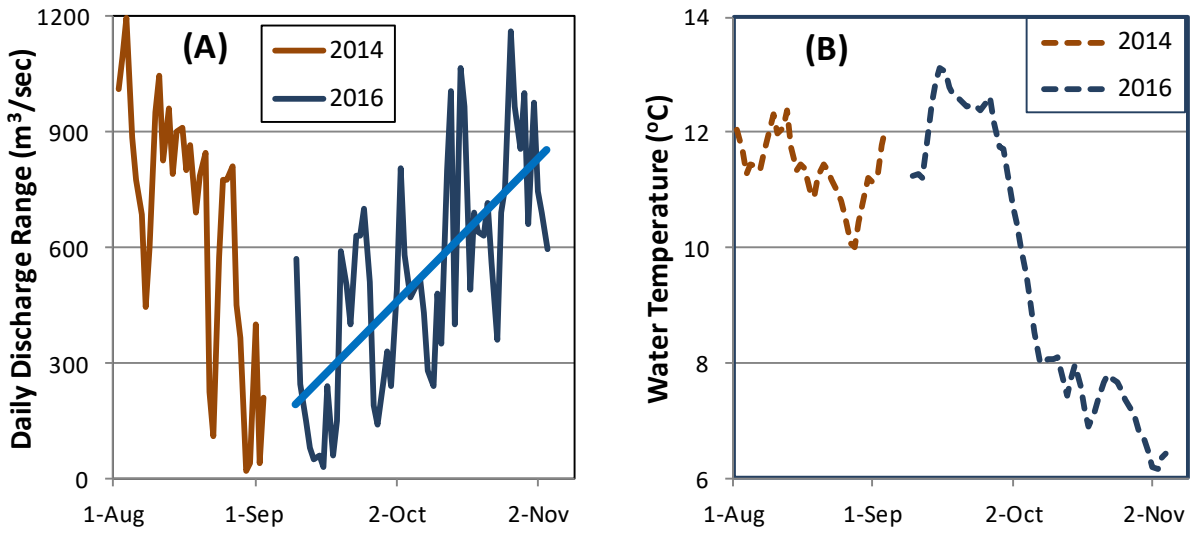

Figure 5: (A) Daily difference between maximum and minimum hourly discharges at the Peace River above the Pine River for 2014 and 2016 periods of interest along with the time trend of daily discharge range (light blue). (B) Water temperature at the Peace River downstream of Moberly River confluence (MobDN1), for 2014 and 2016 periods of interest (dark colours).

2.4.4 Discussion

More detailed exploration of the underlying mechanisms would be interesting but less important in the decision process than the estimated size of the effect. Work in other systems has provided insight into the mechanisms (Scruton et al. 2008, Korman et al. 2011) and statistical analysis of community composition among sites (Schmutz et al. 2015), providing strong supporting evidence of the reality of the effects observed in the Peace River. Additional studies would be required if changes to the size or timing of hydropeaking were being considered during the operation phase of the Project.

The predicted response to 1000 cms daily discharge variation, relative to constant daily discharge was 3-6 nm, or about 10 to 20% of the overall average increment of 27 nm. There is uncertainty in this measurement, as the measurement precision of instruments increased in steps of about 2.4 nm. Detailed estimates of effect size across a range of temperature and discharge variation, including temperature-discharge interactions, is provided in Appendix B.

2.5 FISH COMMUNITY COMPOSITION (TASK 3D)

There were no planned activities to support the evaluation of the effect of flow fluctuations on fish community composition as part of Mon-17 in 2017. Analysis of the fish community composition will occur in Construction Year 4 (2018), with results reported in early 2019. In 2017, large fish indexing continues to be sampled as part of Mon-2. Task 3d will test Hypothesis 5:

H_5: Species-specific fish density among sites, as a measure of species composition, in the Peace River is independent of the magnitude and timing of flow fluctuations.

2.6 RECRUITMENT (TASK 3E)

There were no planned activities to support the evaluation of the effect of flow fluctuation on species-specific recruitment as part of Mon-17 in 2017. Analysis of the species-specific recruitment will occur in Construction Year 4 (2018), with results reported in early 2019. In 2017, large fish indexing continues to be sampled as part of Mon-2, testing Hypothesis 6:

H_6: Species-specific recruitment is independent of the magnitude and timing of flow fluctuations.

Currently, this hypothesis cannot be tested. However, a preliminary examination of patterns in Mountain Whitefish age-frequency data from 2002 to 2016 suggests that there is variation in cohort strength (Figure 6). In a sequence of age-frequency data, strong cohorts can be recognized as higher than average values that persist across years in a diagonal pattern (Figure 6, top panel). The percent contribution relative to adjacent cohorts for four age classes (ages 4 to 7) of 11 cohorts varies from 53 to 81% (bottom panel, Figure 6). Although the data suggests that variation in year class strength is significant, an association between cohort strength and discharge fluctuation may be difficult to tease out because of uncertainties in the timing of the effects tracked across multiple years. Plausible mechanisms linking discharge fluctuations to recruitment can be formulated for almost any life history stage prior, including egg incubation, over-summer growth and over-winter survival. The statistical approach would include adding one or more time-lag parameters, but with a limited number of observations, these parameters are likely to be poorly defined by the data unless there are large, abrupt changes in discharge regime.

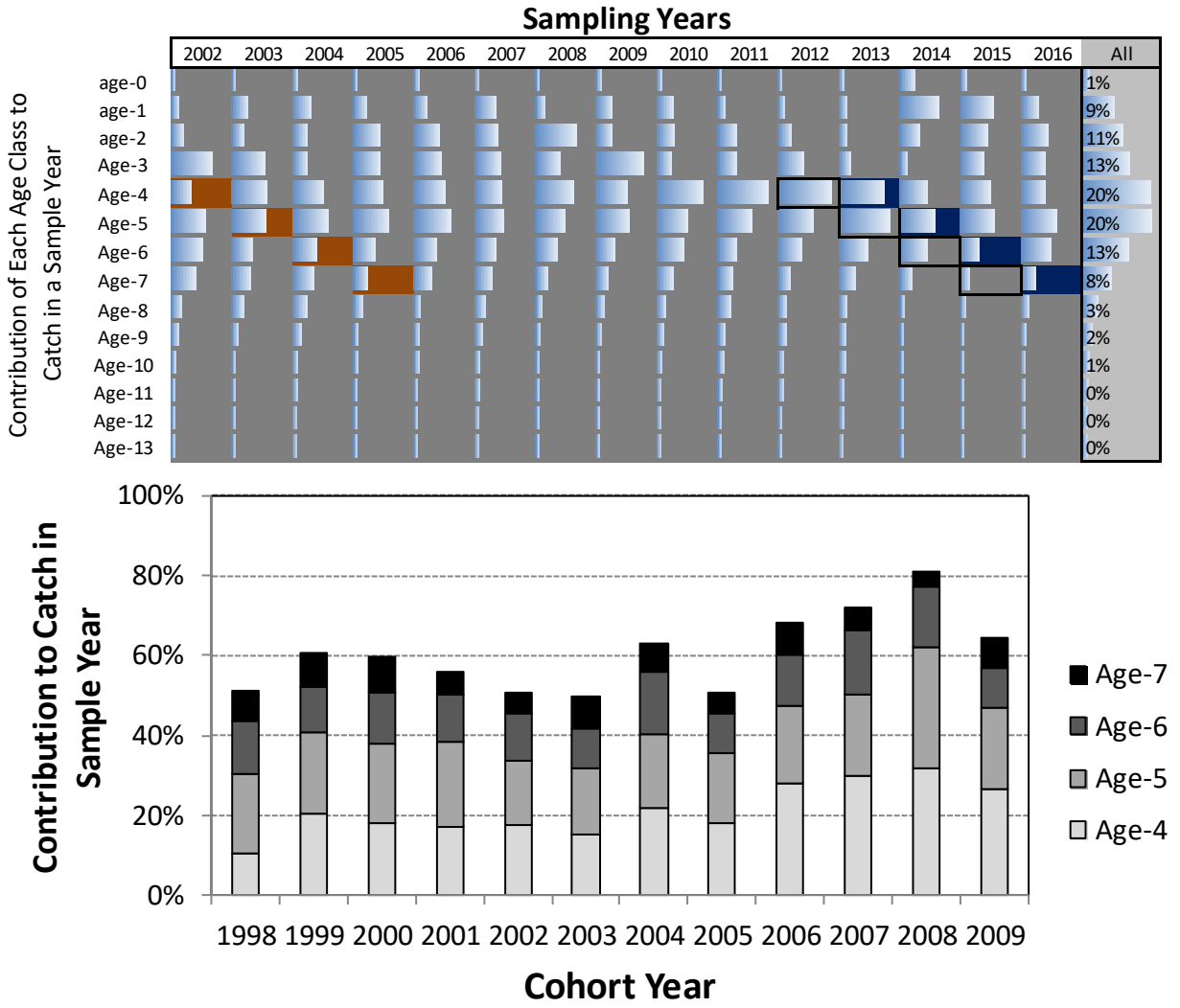

Figure 6: Patterns in the age structure of Mountain Whitefish in large fish index surveys by sample year (top panel) and cohort year (bottom panel). In the top panel, cohort years are highlighted in red (1998), blue (2009) and by boxes (the strong 2008 cohort). The stacked values of diagonals in the top panel represent the contribution of a cohort to the catch, relative to adjacent cohorts (bottom panel). Sample sizes for each year range from 401 in 2002 to 1090 in 2015.

3 SUMMARY (LEARNING)

The Peace River Water Level Fluctuations Monitoring Program (Mon-17) of the Site C FAHMFP examines the effects of flow fluctuations on five performance metrics: fish catchability, benthos and periphyton production, daily growth rate of fish, fish community composition, and fish recruitment. Unlike other monitoring programs, Mon-17 is largely focused on the analysis of data collected as part of other monitoring programs except for the otolith data which are collected as part of Task 2b.

3.1 SUMMARY OF FINDINGS

Question	Answer
What is the context?	Mon-17 evaluates how changes in the Peace River flow regime might affect fish and aquatic habitat and how it is monitored. Unlike other monitoring programs, Mon-17 is analysis-focused, and relies on data collected from other monitoring programs.
What was implemented?	We estimated the effect of flow regime, as measured from Water Survey Station data, on: ▪ **Catchability** – Examined in the large boat electrofishing survey, using data collected between 2004 and 2017 for Mountain Whitefish, Bull Trout, and Arctic Grayling. ▪ **Daily Growth** – Daily growth increments using otoliths collected in 2014 and 2016 based on Mountain Whitefish data. ▪ **Recruitment** – Variation in age class strength using historical age structure data. ▪ Periphyton, benthic invertebrates, and fish community structure were not analyzed this year.
What was the result?	▪ **Catchability,** as measured by catch-per-unit-effort, is independent of flow conditions at the time of sampling for Mountain Whitefish, Bull Trout, and Arctic Grayling. However, a sample year effect was present. For Mountain Whitefish, there is a potential recent decline in abundance after a peak in 2009 to 2011. ▪ **Daily growth** increments were 10-20% lower on days with high flow fluctuations for Mountain Whitefish fry. ▪ **Recruitment** – There was significant variation in age class strength but this cannot be attributed to changes in flow regime.
What was learned?	▪ **Catchability** – Continue evaluating. Potential for further analysis. ▪ **Daily Growth** – Otolith increment data can be used to quantify the effects of flow fluctuation, temperature and perhaps other factors affected by the Project. ▪ **Recruitment** – Mountain Whitefish age class strength varied significantly (i.e., high process error) which will make it difficult to quantify the before and after effect of the Project.

3.2 NEXT STEPS

3.2.1 Catchability (Task 3a)

No changes or additions to sampling protocols are recommended. Continued monitoring and analysis of the relationship between flow fluctuations and catchability of Peace River fish is planned as part of baseline and post-construction monitoring. Additional analyses covering other geographic areas (Sections 6, 7, and 9) are possible for future comparison and/or corroboration of the statements made in this analysis as more data become available. The current monitoring and analysis schedule for Task 3a can be found in Table 2.

Other parameters that may affect catchability should be integrated directly into future analyses. In general terms, this will involve the substitution of a more general function H_{ijk} in place of D_{ij} in Equation 1:

$$C_{ijk} = q_{ijk} N Y_i \text{ where } q_{ijk} = q H_{ijk} \text{ and } H_{ijk} = f(h) \quad \text{Equation 2}$$

where i is a year index, j is a sampling day index, k is a site index and H_{ijk} is a function of h_{ijk}, which is a vector of habitat variables that describes sampling conditions for each sampling event. H_{ijk} can range from 1 (sampling conditions have no effect on C_{ijk}) to a complex function of habitat variables. Habitat variables that are being considered include discharge patterns during and prior to the sampling period and physical characteristics of sites, such as slope or substrate. In the statistical model, h_{ijk} will be transformed into an orthogonal vector using Principle Components Analysis (or a similar approach) to eliminate correlations among habitat characteristics such as discharge on sequential days or substrate and slope.

In this type of analysis, uncertainties in q are explicitly modeled as part of the process of detecting trends in Y_i to disentangle real changes in the population from the effects of variable sampling conditions.

Furthermore, additional analyses of the CPUE data could be performed by disaggregating the CPUE in time within a day rather than the daily average approach taken for our analysis. This method would increase the resolution of the data on CPUE, linking it to the discharge at the time of a sampling bout. However, this approach relies on the spatial location of where catches occurred relative to the hydrometric stations, and the analysis should account for a time lag in the discharge data relative to the location of the sampling bout.

3.2.2 Benthos and Periphyton (Task 3b)

Benthos and periphyton analysis will occur in 2018. The current monitoring and analysis schedule for Task 3b can be found in Table 2**.**

3.2.3 Daily Growth (Task 3c)

Daily growth analysis will occur in 2018. Results from additional years and species are needed to generalize the conclusions from the 2016/17 data collection and analysis. Low resolution may limit the application of this technique to slower growing species, such as sculpins. The current monitoring and analysis schedule for Task 3c can be found in Table 2**.**

Information from this task will contribute to a weight of evidence assessment of the effect of the Project on the downstream ecosystem. Observations of otolith growth rates are difficult to translate into performance measures that are more tightly linked to societal values such as ecosystem productivity, survival rates and adult population density by species.

3.2.4 Fish Community Composition (Task 3d)

Fish community composition analysis will occur in 2018. The current monitoring and analysis schedule for Task 3d can be found in Table 2.

3.2.5 Recruitment (Task 3e)

No changes or additions to sampling plans are recommended. Analysis of existing data suggests that there are variations in cohort strength. However, the nature of the analysis means that degrees of freedom are limited because each measurement involves the demography of a cohort over several years. The most powerful statistical test will be a before/after comparison that can only be done after 10 or more years of operation. The current monitoring and analysis schedule for Task 3e can be found in Table 2.

The potential for future analyses can be illustrated using current data. Age structure provides information on recruitment and survival in three ways: (1) the slope of the descending limb of the catch curve represents adult survival; (2) gaps in age class structure is an indicator of periodic recruitment failure; and (3) an abrupt drop in year class abundance that tracks through successive years can be used to estimate the effect of an abrupt change in habitat conditions (i.e., river diversion, reservoir filling). Current data (Figure 7) provides baseline information for all three indicators. The data suggests that Mountain Whitefish fully recruit to the sampling gear at age-5 and that adult mortality rates are constant. Figure 7A illustrates the derivation of adult mortality rates and Figure 7B illustrates the expected patterns under the two types of recruitment failure.

Errors in ageing and sampling bias are the key issues with this type of analysis. The analysis shown in Figure 7A assumes that catchability is constant on the descending limb, but relative changes can still be inferred as long as the bias is constant through time. Ageing errors blur the results of the Figure 7B analysis and may make periodic failures undetectable.

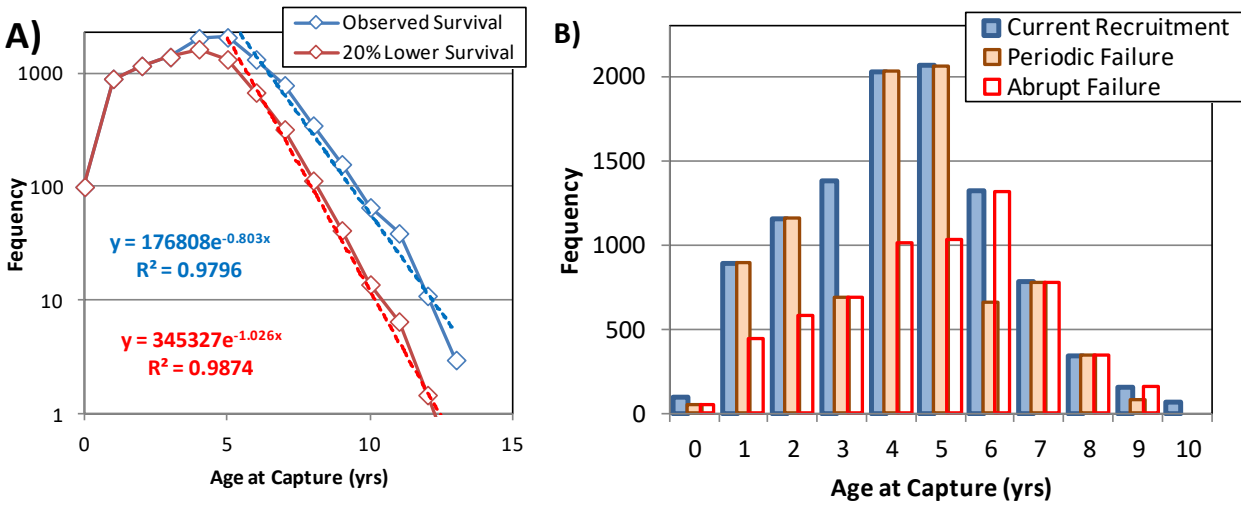

Figure 7: Current age-frequency distribution for Mountain Whitefish sampled between 2003 and 2013 in large fish index surveys *versus* hypothetical distributions representing three alternative mortality changes. A) The slope of the log plot is the instantaneous annual mortality rate (i.e., exp(-(1.026-0.803)) = 1 - 20%= 80%). B) The age-frequency distribution becomes more jagged under periodic recruitment failure. Under an abrupt recruitment failure, the age-frequency distribution becomes steeper in Years 1-4, flatter in Years 5-8 (as in B) before reverting to an approximation of the original shape.

4 REFERENCES

Burnham, K.P. and D.R. Anderson. 2002. “Model Selection and Multimodal Inference: A Practical Information-Theoretic Approach”. 2nd Edition. Springer: New York.

Golder Associates Ltd. and W.J. Gazey Research. 2015. GMSMON-2 Peace Project Water Use Plan – Peace River Fish Index - 2014 Investigations. Report prepared for BC Hydro, Burnaby, British Columbia. Golder Report No. 1400753: 68 p. + 6 app.

Korman, J., Walters, C., Martell, S.J.D., Pine III, W.E. and Dutterer, A., 2011. Effects of flow fluctuations on habitat use and survival of age-0 rainbow trout (Oncorhynchus mykiss) in a large, regulated river. Canadian journal of fisheries and aquatic sciences, 68:1097-1109.

Lyon, J.P., Bird, T., Nicol, S., Kearns, J., O’Mahony, J., Todd, C.R., Cowx, I.G. and Bradshaw, C.J., 2014. Efficiency of electrofishing in turbid lowland rivers: implications for measuring temporal change in fish populations. Canadian Journal of Fisheries and Aquatic Sciences, 71(6), pp.878-886.

Mainstream Aquatics Ltd. 2011. Site C fisheries studies – 2010 Peace River Fish Inventory. Prepared for B.C. Hydro Site C Project, Corporate Affairs Report No. 10005F: 102 p. + plates and appendices.

Mainstream Aquatics Ltd. 2012. EIS Volume 2, Appendix O. Site C Clean Energy Project Fish and Fish Habitat Technical Data Report. Pp 226 + Appendices.

Schmutz, S., Bakken, T.H., Friedrich, T., Greimel, F., Harby, A., Jungwirth, M., Melcher, A., Unfer, G. and Zeiringer, B., 2015. Response of fish communities to hydrological and morphological alterations in hydropeaking rivers of Austria. River research and applications, 31(8), pp.919-930.

Scruton, D.A., Pennell, C., Ollerhead, L.M.N., Alfredsen, K., Stickler, M., Harby, A., Robertson, M., Clarke, K.D. and LeDrew, L.J., 2008. A synopsis of ‘hydropeaking’studies on the response of juvenile Atlantic salmon to experimental flow alteration. Hydrobiologia, 609:263-275.

Speas, D.W., Walters, C.J., Ward, D.L. and Rogers, R.S., 2004. Effects of intraspecific density and environmental variables on electrofishing catchability of brown and rainbow trout in the Colorado River. North American Journal of Fisheries Management, 24(2), pp.586-596.

APPENDIX A: STATISTICAL MODEL OUTPUTS

Mountain Whitefish CPUE #/s

Model 5: (Best fit model)

```
Call:
lm(formula = y_var ~ as.numeric(SampleYear) + as.numeric(SampleYear2),
    data = data1)

Residuals:
    Min      1Q  Median      3Q     Max
-0.7860 -0.1535  0.0226  0.1827  0.6728

Coefficients:
                          Estimate Std. Error t value Pr(>|t|)
(Intercept)             -6.251e+04  6.267e+03  -9.974   <2e-16 ***
as.numeric(SampleYear)   6.224e+01  6.234e+00   9.984   <2e-16 ***
as.numeric(SampleYear2) -1.549e-02  1.550e-03  -9.995   <2e-16 ***
---
Signif. codes:  0 ‘***’ 0.001 ‘**’ 0.01 ‘*’ 0.05 ‘.’ 0.1 ‘ ’ 1

Residual standard error: 0.2705 on 127 degrees of freedom
Multiple R-squared:   0.65,    Adjusted R-squared:  0.6445
F-statistic: 117.9 on 2 and 127 DF,  p-value: < 2.2e-16
```

Model 3:

```
Call:
lm(formula = y_var ~ as.factor(SampleYear), data = data1)

Residuals:
    Min      1Q  Median      3Q     Max
-0.6577 -0.1729  0.0215  0.1669  0.6111

Coefficients:
                           Estimate Std. Error t value Pr(>|t|)
(Intercept)                -2.75525    0.07879 -34.971  < 2e-16 ***
as.factor(SampleYear)2005 -0.00105    0.11417  -0.009  0.99268
as.factor(SampleYear)2007  0.17432    0.11417   1.527  0.12951
as.factor(SampleYear)2008  0.26034    0.11142   2.337  0.02116 *
as.factor(SampleYear)2009  0.18579    0.11142   1.668  0.09809 .
as.factor(SampleYear)2010  0.20858    0.11142   1.872  0.06370 .
as.factor(SampleYear)2011  0.41488    0.11745   3.532  0.00059 ***
as.factor(SampleYear)2012 -0.03252    0.12634  -0.257  0.79734
as.factor(SampleYear)2013 -0.05116    0.13262  -0.386  0.70037
as.factor(SampleYear)2014 -0.10763    0.11745  -0.916  0.36134
as.factor(SampleYear)2015 -0.56288    0.11417  -4.930 2.74e-06 ***
as.factor(SampleYear)2016 -0.66636    0.10705  -6.225 7.78e-09 ***
as.factor(SampleYear)2017 -0.77629    0.10908  -7.117 9.54e-11 ***
---
Signif. codes:  0 ‘***’ 0.001 ‘**’ 0.01 ‘*’ 0.05 ‘.’ 0.1 ‘ ’ 1

Residual standard error: 0.2613 on 117 degrees of freedom
Multiple R-squared:  0.6992,   Adjusted R-squared:  0.6683
F-statistic: 22.66 on 12 and 117 DF,  p-value: < 2.2e-16
```

Model 8:

```
Call:
lm(formula = y_var ~ x1_var + as.numeric(SampleYear) +
as.numeric(SampleYear2),
    data = data1)

Residuals:
     Min       1Q   Median       3Q      Max
```

```
-0.73721 -0.15446  0.02319  0.18949  0.69961

Coefficients:
                          Estimate Std. Error t value Pr(>|t|)
(Intercept)             -6.356e+04  6.354e+03 -10.003   <2e-16 ***
x1_var                   8.303e-05  8.253e-05   1.006    0.316
as.numeric(SampleYear)   6.329e+01  6.321e+00  10.013   <2e-16 ***
as.numeric(SampleYear2) -1.576e-02  1.572e-03 -10.024   <2e-16 ***
---
Signif. codes:  0 ‘***’ 0.001 ‘**’ 0.01 ‘*’ 0.05 ‘.’ 0.1 ‘ ’ 1

Residual standard error: 0.2705 on 126 degrees of freedom
Multiple R-squared:  0.6528,   Adjusted R-squared:  0.6445
F-statistic: 78.97 on 3 and 126 DF,  p-value: < 2.2e-16
```

Mountain Whitefish CPUE #/100m

Model 5: (best fit model)

```
Call:
lm(formula = y2_var ~ as.numeric(SampleYear) + as.numeric(SampleYear2),
    data = data1)

Residuals:
     Min       1Q   Median       3Q      Max
-0.65344 -0.16174  0.04472  0.16875  0.56514

Coefficients:
                          Estimate Std. Error t value Pr(>|t|)
(Intercept)             -4.272e+04  5.776e+03  -7.396 1.68e-11 ***
as.numeric(SampleYear)   4.254e+01  5.746e+00   7.404 1.61e-11 ***
as.numeric(SampleYear2) -1.059e-02  1.429e-03  -7.411 1.55e-11 ***
---
Signif. codes:  0 ‘***’ 0.001 ‘**’ 0.01 ‘*’ 0.05 ‘.’ 0.1 ‘ ’ 1

Residual standard error: 0.2493 on 127 degrees of freedom
Multiple R-squared:  0.4871,   Adjusted R-squared:  0.479
F-statistic:  60.3 on 2 and 127 DF,  p-value: < 2.2e-16
```

Model 3:

```
Call:
lm(formula = y2_var ~ as.factor(SampleYear), data = data1)

Residuals:
     Min       1Q   Median       3Q      Max
-0.63301 -0.14551  0.03045  0.16072  0.55456

Coefficients:
                           Estimate Std. Error t value Pr(>|t|)
(Intercept)                 1.24894    0.07293  17.126  < 2e-16 ***
as.factor(SampleYear)2005   0.05387    0.10568   0.510  0.61116
as.factor(SampleYear)2007   0.20047    0.10568   1.897  0.06031 .
as.factor(SampleYear)2008   0.25638    0.10313   2.486  0.01434 *
as.factor(SampleYear)2009   0.18739    0.10313   1.817  0.07179 .
as.factor(SampleYear)2010   0.12949    0.10313   1.256  0.21178
as.factor(SampleYear)2011   0.29912    0.10871   2.751  0.00688 **
as.factor(SampleYear)2012  -0.05076    0.11694  -0.434  0.66505
as.factor(SampleYear)2013  -0.06168    0.12275  -0.502  0.61631
as.factor(SampleYear)2014   0.14460    0.10871   1.330  0.18608
as.factor(SampleYear)2015  -0.27673    0.10568  -2.619  0.01000 **
as.factor(SampleYear)2016  -0.41648    0.09909  -4.203 5.17e-05 ***
as.factor(SampleYear)2017  -0.48240    0.10096  -4.778 5.19e-06 ***
---
Signif. codes:  0 ‘***’ 0.001 ‘**’ 0.01 ‘*’ 0.05 ‘.’ 0.1 ‘ ’ 1

Residual standard error: 0.2419 on 117 degrees of freedom
Multiple R-squared:  0.5553,   Adjusted R-squared:  0.5096
F-statistic: 12.17 on 12 and 117 DF,  p-value: 1.074e-15
```

Model 6:

```
Call:
lm(formula = y2_var ~ x1_var + as.factor(SampleYear), data = data1)

Residuals:
     Min       1Q   Median       3Q      Max
-0.63006 -0.14994  0.02878  0.14775  0.59180

Coefficients:
                            Estimate Std. Error t value Pr(>|t|)
```

```
(Intercept)                1.3788260  0.1211305  11.383  < 2e-16 ***
x1_var                    -0.0001515  0.0001130  -1.340  0.18275
as.factor(SampleYear)2005  0.0874611  0.1082633   0.808  0.42083
as.factor(SampleYear)2007  0.2373059  0.1088506   2.180  0.03127 *
as.factor(SampleYear)2008  0.3016011  0.1081810   2.788  0.00620 **
as.factor(SampleYear)2009  0.2147743  0.1047966   2.049  0.04267 *
as.factor(SampleYear)2010  0.0875418  0.1074443   0.815  0.41688
as.factor(SampleYear)2011  0.3797949  0.1239414   3.064  0.00271 **
as.factor(SampleYear)2012 -0.0386790  0.1168956  -0.331  0.74133
as.factor(SampleYear)2013 -0.0089448  0.1285088  -0.070  0.94463
as.factor(SampleYear)2014  0.1397808  0.1084049   1.289  0.19981
as.factor(SampleYear)2015 -0.2819232  0.1053948  -2.675  0.00855 **
as.factor(SampleYear)2016 -0.3489586  0.1108598  -3.148  0.00209 **
as.factor(SampleYear)2017 -0.4090144  0.1145519  -3.571  0.00052 ***
---
Signif. codes:  0 ‘***’ 0.001 ‘**’ 0.01 ‘*’ 0.05 ‘.’ 0.1 ‘ ’ 1

Residual standard error: 0.2411 on 116 degrees of freedom
Multiple R-squared:  0.562,    Adjusted R-squared:  0.513
F-statistic: 11.45 on 13 and 116 DF,  p-value: 1.691e-15
```

Model 8:

```
Call:
lm(formula = y2_var ~ x1_var + as.numeric(SampleYear) +
as.numeric(SampleYear2),
    data = data1)

Residuals:
     Min       1Q   Median       3Q      Max
-0.64491 -0.16075  0.04869  0.16789  0.55858

Coefficients:
                          Estimate Std. Error t value Pr(>|t|)
(Intercept)             -4.246e+04  5.878e+03  -7.224 4.24e-11 ***
x1_var                  -2.030e-05  7.634e-05  -0.266    0.791
as.numeric(SampleYear)   4.228e+01  5.847e+00   7.231 4.09e-11 ***
as.numeric(SampleYear2) -1.052e-02  1.454e-03  -7.238 3.94e-11 ***
---
Signif. codes:  0 ‘***’ 0.001 ‘**’ 0.01 ‘*’ 0.05 ‘.’ 0.1 ‘ ’ 1

Residual standard error: 0.2502 on 126 degrees of freedom
Multiple R-squared:  0.4874,   Adjusted R-squared:  0.4752
F-statistic: 39.93 on 3 and 126 DF,  p-value: < 2.2e-16
```

Bull Trout CPUE (#/s)

Model 3:

```
Call:
lm(formula = y_var ~ as.factor(SampleYear), data = data1)

Residuals:
     Min       1Q   Median       3Q      Max
-1.08343 -0.34141 -0.01867  0.33355  0.95362

Coefficients:
                           Estimate Std. Error t value Pr(>|t|)
(Intercept)               -7.211e+00  1.383e-01 -52.157  < 2e-16 ***
as.factor(SampleYear)2005  2.970e-01  2.061e-01   1.441 0.152468
as.factor(SampleYear)2007  5.651e-01  2.004e-01   2.820 0.005682 **
as.factor(SampleYear)2008  8.295e-01  2.004e-01   4.140 6.79e-05 ***
as.factor(SampleYear)2009  4.115e-01  2.004e-01   2.054 0.042364 *
as.factor(SampleYear)2010 -4.619e-05  2.061e-01   0.000 0.999822
as.factor(SampleYear)2011  7.295e-01  2.061e-01   3.539 0.000587 ***
as.factor(SampleYear)2012  5.110e-01  2.217e-01   2.305 0.023045 *
as.factor(SampleYear)2013  5.651e-01  2.327e-01   2.428 0.016783 *
as.factor(SampleYear)2014 -1.765e-01  2.061e-01  -0.856 0.393754
as.factor(SampleYear)2015  1.885e-01  2.004e-01   0.941 0.348895
as.factor(SampleYear)2016  8.542e-01  1.879e-01   4.547 1.40e-05 ***
as.factor(SampleYear)2017  3.592e-01  1.955e-01   1.837 0.068855 .
---
Signif. codes:  0 ‘***’ 0.001 ‘**’ 0.01 ‘*’ 0.05 ‘.’ 0.1 ‘ ’ 1

Residual standard error: 0.4586 on 111 degrees of freedom
Multiple R-squared:  0.3538,   Adjusted R-squared:  0.2839
F-statistic: 5.064 on 12 and 111 DF,  p-value: 1.118e-06
```

Model 6:

```
Call:
lm(formula = y_var ~ x1_var + as.factor(SampleYear), data = data1)

Residuals:
     Min       1Q   Median       3Q      Max
-1.09296 -0.30701 -0.00683  0.32372  0.98761

Coefficients:
                           Estimate Std. Error t value Pr(>|t|)
(Intercept)               -7.4049428  0.2311936 -32.029  < 2e-16 ***
x1_var                     0.0002257  0.0002162   1.044 0.298710
as.factor(SampleYear)2005  0.2508907  0.2107003   1.191 0.236316
as.factor(SampleYear)2007  0.5102265  0.2070664   2.464 0.015285 *
as.factor(SampleYear)2008  0.7593561  0.2112624   3.594 0.000488 ***
as.factor(SampleYear)2009  0.3713661  0.2039326   1.821 0.071321 .
as.factor(SampleYear)2010  0.0603935  0.2140061   0.282 0.778317
as.factor(SampleYear)2011  0.6092878  0.2360084   2.582 0.011148 *
as.factor(SampleYear)2012  0.4929862  0.2222960   2.218 0.028631 *
as.factor(SampleYear)2013  0.4865468  0.2445047   1.990 0.049080 *
as.factor(SampleYear)2014 -0.1692876  0.2061438  -0.821 0.413302
as.factor(SampleYear)2015  0.1962166  0.2004200   0.979 0.329715
as.factor(SampleYear)2016  0.7535949  0.2110628   3.570 0.000530 ***
as.factor(SampleYear)2017  0.2503039  0.2215582   1.130 0.261042
---
Signif. codes:  0 ‘***’ 0.001 ‘**’ 0.01 ‘*’ 0.05 ‘.’ 0.1 ‘ ’ 1

Residual standard error: 0.4584 on 110 degrees of freedom
Multiple R-squared:  0.3601,   Adjusted R-squared:  0.2845
F-statistic: 4.763 on 13 and 110 DF,  p-value: 1.675e-06
```

Bull Trout CPUE (#/100m)

Model 3: (Best fit model)

```
Call:
lm(formula = y_var2 ~ as.factor(SampleYear), data = data1)

Residuals:
     Min       1Q   Median       3Q      Max
-0.95839 -0.31776  0.00262  0.33518  0.86331

Coefficients:
                          Estimate Std. Error t value Pr(>|t|)
(Intercept)               -3.17909    0.13042 -24.377  < 2e-16 ***
as.factor(SampleYear)2005  0.33067    0.19441   1.701  0.09177 .
as.factor(SampleYear)2007  0.56306    0.18899   2.979  0.00355 **
as.factor(SampleYear)2008  0.79006    0.18899   4.180 5.83e-05 ***
as.factor(SampleYear)2009  0.40147    0.18899   2.124  0.03586 *
as.factor(SampleYear)2010 -0.04779    0.19441  -0.246  0.80628
as.factor(SampleYear)2011  0.60076    0.19441   3.090  0.00253 **
as.factor(SampleYear)2012  0.46224    0.20913   2.210  0.02914 *
as.factor(SampleYear)2013  0.51682    0.21952   2.354  0.02032 *
as.factor(SampleYear)2014  0.03237    0.19441   0.167  0.86805
as.factor(SampleYear)2015  0.42800    0.18899   2.265  0.02548 *
as.factor(SampleYear)2016  1.05476    0.17720   5.952 3.15e-08 ***
as.factor(SampleYear)2017  0.60507    0.18444   3.281  0.00138 **
---
Signif. codes:  0 ‘***’ 0.001 ‘**’ 0.01 ‘*’ 0.05 ‘.’ 0.1 ‘ ’ 1

Residual standard error: 0.4325 on 111 degrees of freedom
Multiple R-squared:  0.3797,   Adjusted R-squared:  0.3126
F-statistic: 5.662 on 12 and 111 DF,  p-value: 1.614e-07
```

Model 6:

```
Call:
lm(formula = y_var2 ~ x1_var + as.factor(SampleYear), data = data1)

Residuals:
     Min       1Q   Median       3Q      Max
-0.96271 -0.31462  0.00313  0.31718  0.87907

Coefficients:
                            Estimate Std. Error t value Pr(>|t|)
(Intercept)               -3.2668117  0.2188992 -14.924  < 2e-16 ***
x1_var                     0.0001023  0.0002047   0.500 0.618141
as.factor(SampleYear)2005  0.3097881  0.1994957   1.553 0.123330
as.factor(SampleYear)2007  0.5381831  0.1960550   2.745 0.007068 **
as.factor(SampleYear)2008  0.7582477  0.2000278   3.791 0.000246 ***
as.factor(SampleYear)2009  0.3832944  0.1930879   1.985 0.049625 *
as.factor(SampleYear)2010 -0.0203903  0.2026257  -0.101 0.920027
as.factor(SampleYear)2011  0.5462771  0.2234579   2.445 0.016087 *
as.factor(SampleYear)2012  0.4540814  0.2104747   2.157 0.033149 *
as.factor(SampleYear)2013  0.4812067  0.2315024   2.079 0.039978 *
as.factor(SampleYear)2014  0.0356280  0.1951814   0.183 0.855497
as.factor(SampleYear)2015  0.4315039  0.1897620   2.274 0.024911 *
as.factor(SampleYear)2016  1.0091592  0.1998388   5.050 1.77e-06 ***
as.factor(SampleYear)2017  0.5556883  0.2097761   2.649 0.009262 **
---
Signif. codes:  0 ‘***’ 0.001 ‘**’ 0.01 ‘*’ 0.05 ‘.’ 0.1 ‘ ’ 1

Residual standard error: 0.434 on 110 degrees of freedom
Multiple R-squared:  0.3811,   Adjusted R-squared:  0.308
```

Arctic Grayling CPUE #/s

Model 7 (best model):

```
Call:
lm(formula = y_var ~ x1_var + as.numeric(SampleYear), data = data1)

Residuals:
     Min       1Q   Median       3Q      Max
-2.38200 -0.36303 -0.01986  0.31330  1.89378

Coefficients:
                         Estimate Std. Error t value Pr(>|t|)
(Intercept)             3.425e+02  2.931e+01  11.685  < 2e-16 ***
x1_var                  1.048e-03  2.102e-04   4.985 2.21e-06 ***
as.numeric(SampleYear) -1.742e-01  1.461e-02 -11.920  < 2e-16 ***
---
Signif. codes:  0 ‘***’ 0.001 ‘**’ 0.01 ‘*’ 0.05 ‘.’ 0.1 ‘ ’ 1

Residual standard error: 0.6331 on 115 degrees of freedom
Multiple R-squared:  0.5563,   Adjusted R-squared:  0.5486
F-statistic: 72.08 on 2 and 115 DF,  p-value: < 2.2e-16
```

Model 3 (next best model):

```
Call:
lm(formula = y_var ~ as.factor(SampleYear), data = data1)

Residuals:
     Min       1Q   Median       3Q      Max
-1.88705 -0.32843 -0.01998  0.31422  1.90805

Coefficients:
                           Estimate Std. Error t value Pr(>|t|)
(Intercept)                 -5.9559     0.1850 -32.202  < 2e-16 ***
as.factor(SampleYear)2005    0.3793     0.2680   1.415 0.160025
as.factor(SampleYear)2007    0.4887     0.2680   1.823 0.071102 .
as.factor(SampleYear)2008    0.1047     0.2616   0.400 0.689857
as.factor(SampleYear)2009   -0.6965     0.2616  -2.663 0.008968 **
as.factor(SampleYear)2010   -0.9922     0.2680  -3.702 0.000343 ***
as.factor(SampleYear)2011   -0.4576     0.2757  -1.660 0.099964 .
as.factor(SampleYear)2012   -1.0742     0.3113  -3.450 0.000807 ***
as.factor(SampleYear)2013   -1.0519     0.3582  -2.937 0.004073 **
as.factor(SampleYear)2014   -1.9309     0.3309  -5.836 6.01e-08 ***
as.factor(SampleYear)2015   -1.7082     0.2757  -6.196 1.15e-08 ***
as.factor(SampleYear)2016   -1.1137     0.2616  -4.258 4.51e-05 ***
as.factor(SampleYear)2017   -1.3898     0.2616  -5.314 6.07e-07 ***
---
Signif. codes:  0 ‘***’ 0.001 ‘**’ 0.01 ‘*’ 0.05 ‘.’ 0.1 ‘ ’ 1

Residual standard error: 0.6134 on 105 degrees of freedom
Multiple R-squared:  0.6197,   Adjusted R-squared:  0.5762
F-statistic: 14.26 on 12 and 105 DF,  p-value: < 2.2e-16
```

Model 8:

```
Call:
lm(formula = y_var ~ x1_var + as.numeric(SampleYear) +
as.numeric(SampleYear2),
    data = data1)

Residuals:
     Min       1Q   Median       3Q      Max
-2.36914 -0.36649 -0.01924  0.31284  1.88663

Coefficients:
```

```
                          Estimate Std. Error t value Pr(>|t|)
(Intercept)             -1.713e+03  1.541e+04  -0.111    0.912
x1_var                   1.053e-03  2.144e-04   4.909 3.07e-06 ***
as.numeric(SampleYear)   1.871e+00  1.533e+01   0.122    0.903
as.numeric(SampleYear2) -5.085e-04  3.812e-03  -0.133    0.894
---
Signif. codes:  0 ‘***’ 0.001 ‘**’ 0.01 ‘*’ 0.05 ‘.’ 0.1 ‘ ’ 1

Residual standard error: 0.6358 on 114 degrees of freedom
Multiple R-squared:  0.5563,   Adjusted R-squared:  0.5447
F-statistic: 47.65 on 3 and 114 DF,  p-value: < 2.2e-16
```

Arctic Grayling CPUE #/100m

Model 3: (Best fit model)

```
Call:
lm(formula = y2_var ~ as.factor(SampleYear), data = data1)

Residuals:
     Min       1Q   Median       3Q      Max
-1.78575 -0.33313 -0.00531  0.26769  1.80993

Coefficients:
                          Estimate Std. Error t value Pr(>|t|)
(Intercept)                -1.9819     0.1791 -11.067  < 2e-16 ***
as.factor(SampleYear)2005   0.4281     0.2595   1.649 0.102043
as.factor(SampleYear)2007   0.5164     0.2595   1.990 0.049215 *
as.factor(SampleYear)2008   0.1071     0.2533   0.423 0.673177
as.factor(SampleYear)2009  -0.6712     0.2533  -2.650 0.009292 **
as.factor(SampleYear)2010  -1.0339     0.2595  -3.984 0.000125 ***
as.factor(SampleYear)2011  -0.5501     0.2670  -2.061 0.041800 *
as.factor(SampleYear)2012  -1.0629     0.3014  -3.526 0.000626 ***
as.factor(SampleYear)2013  -1.0429     0.3468  -3.007 0.003300 **
as.factor(SampleYear)2014  -1.6913     0.3204  -5.279 7.04e-07 ***
as.factor(SampleYear)2015  -1.4423     0.2670  -5.402 4.13e-07 ***
as.factor(SampleYear)2016  -0.8985     0.2533  -3.548 0.000583 ***
as.factor(SampleYear)2017  -1.1009     0.2533  -4.347 3.21e-05 ***
---
Signif. codes:  0 ‘***’ 0.001 ‘**’ 0.01 ‘*’ 0.05 ‘.’ 0.1 ‘ ’ 1

Residual standard error: 0.594 on 105 degrees of freedom
Multiple R-squared:  0.5859,   Adjusted R-squared:  0.5386
F-statistic: 12.38 on 12 and 105 DF,  p-value: 2.56e-15
```

Model 6:

```
Call:
lm(formula = y2_var ~ x1_var + as.factor(SampleYear), data = data1)

Residuals:
     Min       1Q   Median       3Q      Max
-1.85197 -0.29814 -0.02298  0.26154  1.74131

Coefficients:
                            Estimate Std. Error t value Pr(>|t|)
(Intercept)               -2.2541229  0.3447226  -6.539 2.36e-09 ***
x1_var                     0.0003175  0.0003435   0.924 0.357375
as.factor(SampleYear)2005  0.3576709  0.2706340   1.322 0.189200
as.factor(SampleYear)2007  0.4391749  0.2728007   1.610 0.110457
as.factor(SampleYear)2008  0.0123396  0.2733952   0.045 0.964086
as.factor(SampleYear)2009 -0.7285732  0.2609375  -2.792 0.006233 **
as.factor(SampleYear)2010 -0.9481869  0.2757599  -3.438 0.000843 ***
```

```
as.factor(SampleYear)2011 -0.7192438  0.3237679  -2.221 0.028486 *
as.factor(SampleYear)2012 -1.0912961  0.3032107  -3.599 0.000491 ***
as.factor(SampleYear)2013 -1.1442621  0.3639589  -3.144 0.002173 **
as.factor(SampleYear)2014 -1.6755172  0.3210345  -5.219 9.24e-07 ***
as.factor(SampleYear)2015 -1.4414973  0.2671524  -5.396 4.31e-07 ***
as.factor(SampleYear)2016 -1.0812407  0.3214144  -3.364 0.001077 **
as.factor(SampleYear)2017 -1.2541083  0.3028410  -4.141 7.05e-05 ***
---
Signif. codes:  0 ‘***’ 0.001 ‘**’ 0.01 ‘*’ 0.05 ‘.’ 0.1 ‘ ’ 1

Residual standard error: 0.5944 on 104 degrees of freedom
Multiple R-squared:  0.5893,   Adjusted R-squared:  0.5379
F-statistic: 11.48 on 13 and 104 DF,  p-value: 6.258e-15
```

APPENDIX B: 2016 JUVENILE OTOLITH DAILY GROWTH ANALYSIS

TECHNICAL MEMORANDUM

Date: 7 May 2018
To: Brent Mossop, BC Hydro
CC: Dustin Ford (Golder)
From: Sima Usvyatsov, PhD
Tanya Seebacher, MSc, RPBio

Reference No. 1668064-003-TM-Rev1

e-mail: Sima_Usvyatsov@golder.com
Tanya_Seebacher@golder.com

1.0 BACKGROUND

The construction and operation of the Site C Clean Energy Project (the Project) is expected the change the typical daily hydrograph for the Peace River downstream of the Project, which could affect fish populations by altering the amount or quality of fish habitat, potentially influencing fish growth or survival. As summarized in the Peace River Water Levels Fluctuations Monitoring Program (Mon-17) of the Site C Fisheries and Aquatic Habitat Monitoring and Follow-up Program (FAHMFP), the Project will result in the following changes to the Peace River downstream of the Project:

> *During Project operation, daily discharge fluctuations are expected to increase and phase shifted to different times of the day. The daily range of water levels is predicted to increase from 0.5 m to 1.0 m at the Site C tailrace, increase from 0.4 m to 0.8 m near Taylor, BC, and increase from 0.5 to 0.9 m near the Alces River confluence. While operations at Peace Canyon can vary based on a number of factors, there are at times daily patterns in the operations. For example, the following summary is based on information from summer (July 20 to Sept 20 to capture the period when fish sampling typically occurs) discharge during 2014 (high flow) and 2015 (low flow). During these time periods, daily peak Peace River discharge at the Taylor gauge typically occurs between 2:00 am and 6:00 am but during Site C operations the daily pattern is expected to be similar to the current Hudson's Hope hydrograph, which typically peaks between 2:00 pm and 6:00 pm. However, these patterns were not consistent. Flows at the Alces River confluence currently lag those at Taylor by approximately 5 to 6 hours. Peak flows at the Alces River confluence are expected to shift from between 7:00 am and 12:00 pm to 7:00 pm and 12:00 am.*

In 2016, BC Hydro commissioned Golder Associates Ltd. (Golder) to collect and measure the widths of daily growth rings on otoliths collected from juvenile Peace River fishes and examine the effects of discharge variability (m^3/s) on daily incremental otolith growth (µm). These activities correspond to Task 2b of Mon-17. Information collected as part of Task 2b will be used to answer Mon 17's second management question:

2) How do changes in the hydrological regime affect fish and fish habitat of the Peace River?

1.1 Objectives

The main objective of Mon-17 is to address uncertainties regarding hydrographic changes in the Peace River as a result of the Project's construction and operation. Task 2b is designed to test the following Mon-17 management hypothesis:

> H_4: Species-specific fish growth of age-0 and age-1 fish among sites in the Peace River is independent of the magnitude and timing of flow fluctuations.

To address this objective, otolith daily growth rings collected from small (age-0 and age-1) indicator species fish were compared to flow history up to approximately 50 days prior to sampling, where possible.

2.0 METHODS

2.1 Fish Growth

2.1.1 Field Collections

On 4 November 2016, Golder collected juvenile fish from the Peace River at several locations between the Site C dam site and the Pine River confluence. This area of the Peace River is expected to experience the largest variation in water levels associated with Project. Fish were collected in November (i.e., near the end of the growing season) because daily growth rings were expected to be more readily visible on otoliths during the preceding months. Additionally, discharge variability was high during this period.

The 2-person crew attempted to collect all fish encountered while using a Smith-Root Inc. high-output Generator Powered Pulsator (GPP 5.0) electroshocker operated out of a 200 HP outboard jet-drive riverboat, a Smith-Root Inc. LR24 backpack electrofishing unit, and a 5 m wide beach seine (3 mm mesh size). Sampling was limited to portions of the river immediately adjacent to the shoreline, and within the varial zone when possible, as these areas were expected to experience the greatest changes in habitat due to water level fluctuations. The crew captured 6 Arctic Grayling (*Thymallus arcticus*), 4 Longnose Sucker (*Catostomus catostomus*), 77 Mountain Whitefish (*Prosopium williamsoni*), 1 Northern Pike (*Esox lucius*) and 1 Rainbow Trout (*Oncorhynchus mykiss*). All fish were captured between the Site C dam site the Pine River confluence. All 89 fish were small enough to be considered age-0. After collection, fish were euthanized using a diluted clove oil bath. Once mortality was confirmed, each fish was measured for fork length (FL; mm), weighed (g), and stored in labeled plastic bags in a cooler of ice. Sagittal otoliths were removed in the laboratory using the techniques described in Schneidervin and Hubert (1986). Scissors were used to cut the gill arch, isthmus and approximately 75% of the way through the roof of the fish's mouth. The backbone was broken downwards to expose the otoliths and fine-point forceps were used to remove the otoliths. The membranous sac was manually removed from around each otolith and each pair of otoliths was placed in a single labelled envelope and left to dry.

In addition to the dataset detailed above, three age-1 Mountain Whitefish that were collected during the Peace Project Water Use Plan's 2014 Peace River Fish Index (Golder and Gazey 2015) were included in the analysis to provide insight into the effect of discharge variability on growth of age-1 fish.

2.1.2 Laboratory Analysis

Otolith samples were provided to the Okanagan Nation Alliance (ONA) fish ageing laboratory in Westbank, BC for daily circuli measurements. Otoliths were embedded in epoxy and a central transverse section, approximately 0.5 mm thick, was cut on an Isomet low-speed saw. The sections were mounted on glass slides and a calibrated image was taken under phase-contrast at 40x magnification. The smallest visible growth rings, beginning at the margin and progressing inwards, were marked and measured using Image-Pro Plus 7.0 processing software (Media Cybernetics, MD, USA). Thus, the otolith increment data presented below represent otolith growth extending from day of capture back in time up to approximately 50 days or until no growth increments could be distinguished (range 24 to 56 days). Note that 50 days of growth was set as a target growth period for this study, but growth beyond 50 days was visible on most of the otoliths examined. The analysis could likely be expanded during future study to include a larger growth period if necessary.

2.2 Discharge

2.2.1 Data Collection

Hourly discharge (m^3/s) data were obtained from the Government of Canada (Water Office) from station #07FA004 (Peace River above the Pine River). Hourly water temperature data collected from Moberly River (stations mobDN1 and mobDN2) were used where water temperature was included as a variable in analysis.

2.2.2 Data Processing

Hourly discharge data were used to calculate daily discharge range (the difference between daily maximum and minimum discharges; m^3/s). Hourly water temperatures were used to calculate mean daily temperature. Discharge and temperature data were then linked to otolith growth. The interpretation of otolith growth rings is that the first outward opaque ring was deposited the night before capture, and therefore the distance between the first 2 most outward opaque rings represents the previous day's growth. However, it is not known whether changes in environmental variables affect growth on the same day or whether there is a delay between changes to discharge (or temperature) and the deposition of otolith rings. Therefore, the analysis included several sets of candidate models that included a time lag between environmental variables and otolith growth. The mean daily temperatures and daily ranges of discharge were calculated for the raw data, as well as data offset by 12 h, 24 h, and 48 h, to account for a time delay in the effect of discharge variability on otolith growth. This resulted in a set of eight statistics of discharge variability for each day of otolith growth.

2.3 Data Analysis

The modeling process was conducted separately for age-0 Mountain Whitefish, age-1 Mountain Whitefish (from the 2014 dataset), and Longnose Sucker to account for age and species differences in otolith growth rates and responses to environmental conditions. Each of these groupings is discussed below.

2.3.1 Age-0 Mountain Whitefish

Daily otolith growth increments were compared to daily discharge variability using repeated-measures linear mixed models. The use of a repeated measures analysis accounted for the individual variability of otolith growth in each sampled fish, as well as incorporated the lack of independence of otolith increment data within specimens. Since growth can be affected by both

water temperature and fish body size, mean daily water temperature values and individual fish fork lengths were used as covariates in the models.

To determine which variables should be included as predictors in the final models, the daily otolith growth increments were used to perform regressions using the following variables:

1) fork length (mm)

2) daily discharge range (m^3/s; the difference between the maximum and minimum hourly discharges within each day);

   a) with no offset

   b) with a 12 h offset

   c) with a 24 h offset

   d) with a 48 h offset

3) quadratic function of mean daily water temperature (ºC);

   a) with no offset

   b) with a 12 h offset

   c) with a 24 h offset

   d) with a 48 h offset

Four mixed-effect models were constructed, with fixed effects of fork length, temperature, and discharge range with the four offsets were constructed, where the fixed effects were comprised of fork length and environmental variables. The mathematic representation of the models is as follows:

1) $$g_{i,j} = \beta_0 + \beta_{1,k} \times \text{Daily discharge range}_{i,k} + \beta_{2,k} \times \text{Mean daily temperature}_{i,k} + \beta_{3,k} \times \text{Mean daily temperature}^2_{i,k} + \beta_4 \times \text{Fork length}_j + \beta_{12,k} \times \text{Daily discharge range}_{i,k} \times \text{Mean daily temperature}_{i,k} + \beta_{13,k} \times \text{Daily discharge range}_{i,k} \times \text{Mean daily temperature}^2_{i,k} + \beta_{14,k} \times \text{Daily discharge range}_{i,k} \times \text{Fork length}_j + \beta_{24,k} \times \text{Mean daily temperature}_{i,k} \times \text{Fork length}_j + \beta_{34,k} \times \text{Mean daily temperature}^2_{i,k} \times \text{Fork length}_j + b_{0j} + b_{1j} \times \text{Daily discharge range}_{i,k} + b_{2j} \times \text{Mean daily temperature}_{i,k} + b_{3j} \times \text{Mean daily temperature}^2_{i,k} + \varepsilon_{i,j}$$

where $g_{i,j}$ is the otolith ring width of the *j*-th fish on day *i*, β_0 is the intercept of each equation, $\beta_{1,k}$ is the effect of daily discharge with the *k*-th offset (0 h, 12 h, 24 h, or 48 h), $\beta_{2,k}$ is the effect of mean daily temperature with the k-th offset, $\beta_{3,k}$ is the quadratic effect of temperature with the *k*-th offset, $\beta_{12,k}$ and $\beta_{13,k}$ are the interaction effects between discharge range and the first and second degree of mean daily temperature, $\beta_{14,k}$ is the interaction between discharge range and fork length of the j-th fish, and $\beta_{24,k}$ and $\beta_{34,k}$ the interaction effects between fork length of the j-th fish and the first and second degree of mean daily temperature, b_{1j} is a random slope of discharge range, b_{2j} and b_{3j} are the random slopes of first and second degree polynomials of water temperature, and $\varepsilon_{i,j}$ is the error term.

At this stage, models were fitted using maximum likelihood to allow comparison of fixed effects for selection of temporal offset. Model selection was conducted using marginal Akaike's Information Criterion, corrected for small sample size (mAICc), where models with the lowest mAICc values were considered to have more support given the collected data. Marginal AIC values can be used for mixed model selection where the goal of the analysis is estimating population-level effects (Vaida and Blanchard 2005). Once the offset was selected, the model

was refitted using three approaches: 1) generalized least squares (i.e., no random effect), 2) random intercept fitted using restricted maximum likelihood (REML), and 2) random intercept and random slopes for additive effects of discharge and quadratic effect of water temperature (also fitted using REML). The three models were compared using likelihood ratio tests to determine the most appropriate structure of the random effects (Zuur et al 2009).
Once the random effect structure was determined, a set of 4 candidate models with the following fixed effects was compared:

1) $g_{i,j} = \beta_0 + \beta_{1,k} \times \text{Daily discharge range}_{i,k} + \beta_{2,k} \times \text{Mean daily temperature}_{i,k} + \beta_{3,k} \times \text{Mean daily temperature}^2_{i,k} + \beta_4 \times \text{Fork length}_j + \beta_{12,k} \times \text{Daily discharge range}_{i,k} \times \text{Mean daily temperature}_{i,k} + \beta_{13,k} \times \text{Daily discharge range}_{i,k} \times \text{Mean daily temperature}^2_{i,k} + \beta_{14,k} \times \text{Daily discharge range}_{i,k} \times \text{Fork length}_j + \beta_{24,k} \times \text{Mean daily temperature}_{i,k} \times \text{Fork length}_j + \beta_{34,k} \times \text{Mean daily temperature}^2_{i,k} \times \text{Fork length}_j$
2) $g_{i,j} = \beta_0 + \beta_{1,k} \times \text{Daily discharge range}_{i,k} + \beta_{2,k} \times \text{Mean daily temperature}_{i,k} + \beta_4 \times \text{Fork length}_j + \beta_{12,k} \times \text{Daily discharge range}_{i,k} \times \text{Mean daily temperature}_{i,k} + \beta_{14,k} \times \text{Daily discharge range}_{i,k} \times \text{Fork length}_j + \beta_{24,k} \times \text{Mean daily temperature}_{i,k} \times \text{Fork length}_j$
3) $g_{i,j} = \beta_0 + \beta_{1,k} \times \text{Daily discharge range}_{i,k} + \beta_{2,k} \times \text{Mean daily temperature}_{i,k} + \beta_{3,k} \times \text{Mean daily temperature}^2_{i,k} + \beta_{12,k} \times \text{Daily discharge range}_{i,k} \times \text{Mean daily temperature}_{i,k} + \beta_{13,k} \times \text{Daily discharge range}_{i,k} \times \text{Mean daily temperature}^2_{i,k}$
4) $g_{i,j} = \beta_0 + \beta_{1,k} \times \text{Daily discharge range}_{i,k} + \beta_{2,k} \times \text{Mean daily temperature}_{i,k} + \beta_{12,k} \times \text{Daily discharge range}_{i,k} \times \text{Mean daily temperature}_{i,k}$

Where model #1 is the original model fitted, which contains all explanatory variables (fork length, discharge, and temperature), and where temperature effect is expressed as a quadratic function. Model #2 contains all explanatory variables, but the effect of temperature is linear. Models #3-4 are the same as models #1-2, but with the removal of fork length as an explanatory variable, leaving only discharge and water temperature. The models were fitted using maximum likelihood and compared using marginal AICc values.
The fit of the final model was evaluated using visual examination of residual plots for normality, linearity, and heteroscedasticity. Due to residual heteroscedasticity, a within-group power heteroscedasticity structure was added to the model, to describe the increase in residuals with an increase in fitted values. An R^2 statistic for fixed effects (Jaeger et al 2016) was calculated for the final model. All analyses were performed in the statistical environment R (v. 3.3.3; R 2017).
The following assumptions were made for the candidate models:

1) Individual daily otolith growth increments do not change with fish age (i.e., the daily deposition of otolith increments does not depend on fish age in the period of interest; July to early November).

2) Otolith growth as a function of temperature or discharge variability may vary individually beyond the effect of fish size (i.e., in fish of the same size, otolith growth rate as a function of temperature or discharge may differ across individuals during the period of interest).

3) Otolith growth is correlated with fish body growth; therefore, effects of flow fluctuations on otolith growth can be interpreted as effects on fish body growth.

The first assumption was required because the age of the captured fish (i.e., days since hatch) could not be determined, and therefore the effect of age on otolith growth rate could not be modeled. While age may strongly influence otolith growth rate in early life stages, the effect decreases with age in the first year of life (e.g., Cotano and Alvarez 2003, Aldanondo et al. 2010). The alternative approach to making the assumption of constant otolith growth during the period of interest, is to assume a common day of hatch for all captured fish. This is a very strong assumption, since hatches can extend over several weeks. This assumption is especially strong for a dataset that spans three years, with variable water temperature regimes, since water temperatures strongly affect the exact timing of the hatching period. However, to provide an alternative to the assumption of constant growth, a model was constructed to examine the effect of day (where day 1 is 20 July) on otolith increment growth.

2.3.2 Age-1 Mountain Whitefish

The modeling process described above for age-0 Mountain Whitefish was repeated for age-1 Mountain Whitefish. However, since only three age-1 fish were included in the analysis, and since their lengths were similar (range of 170 to 175 mm FL), models that included fork lengths in the analysis were omitted. The selection of fixed effects included eight models, where for each time offset (0 h, 12 h, 24 h, and 48 h), two models were constructed: an additive model of discharge range and a quadratic effect of water temperature, and an additive model of discharge range and a linear effect of water temperature. In addition, to avoid overparameterization of the models, no interactions were included in the models. The model of otolith incremental growth with day of study was not examined, since otolith growth is not likely to be affected by age in the period of the study for fish older than age-1.

2.3.3 Longnose Sucker

The modeling process described above for age-0 Mountain Whitefish was repeated for Longnose Sucker. However, since only one Longnose Sucker was included in the analysis, fork lengths and random effects were not included in the models, and the selection of fixed effects included eight models, where for each time offset (0 h, 12 h, 24 h, and 48 h), two models were constructed: an additive model of discharge range and a quadratic effect of water temperature, and an additive model of discharge range and a linear effect of water temperature.

3.0 RESULTS

Otolith samples were analyzed by the ONA's fish ageing laboratory in Westbank, BC. Due to the nature of the analysis, protocols for otolith preparation were not available prior to sampling and were established based on lessons learned while processing the 2016 samples. These protocols should be implemented during future study years to ensure consistency between datasets.

3.1 Discharge

Back-estimated otolith growth data extended from early September to early November, depending on fish species and year. Peace River discharge recorded during the period encompassing the period of daily otolith growth data (August to early November, depending on year) varied within each day, among days within each year, and among years (Figure 8). The time series of variability of daily discharge, expressed as discharge range (i.e., the difference between daily maximum and daily minimum hourly discharges) differed by year (Figure 9). In 2014, variability was high in the beginning of the study period (up to 1,200 m^3/s) and decreased throughout the study period to approximately 600 to 900 m^3/s by mid-September, although multiple days with low variability were recorded throughout the study period. In 2016, discharge ranges were lower in the beginning of the study period (30 to 600 m^3/s) and gradually increased over the study period to 600 to 1,200 m^3/s.

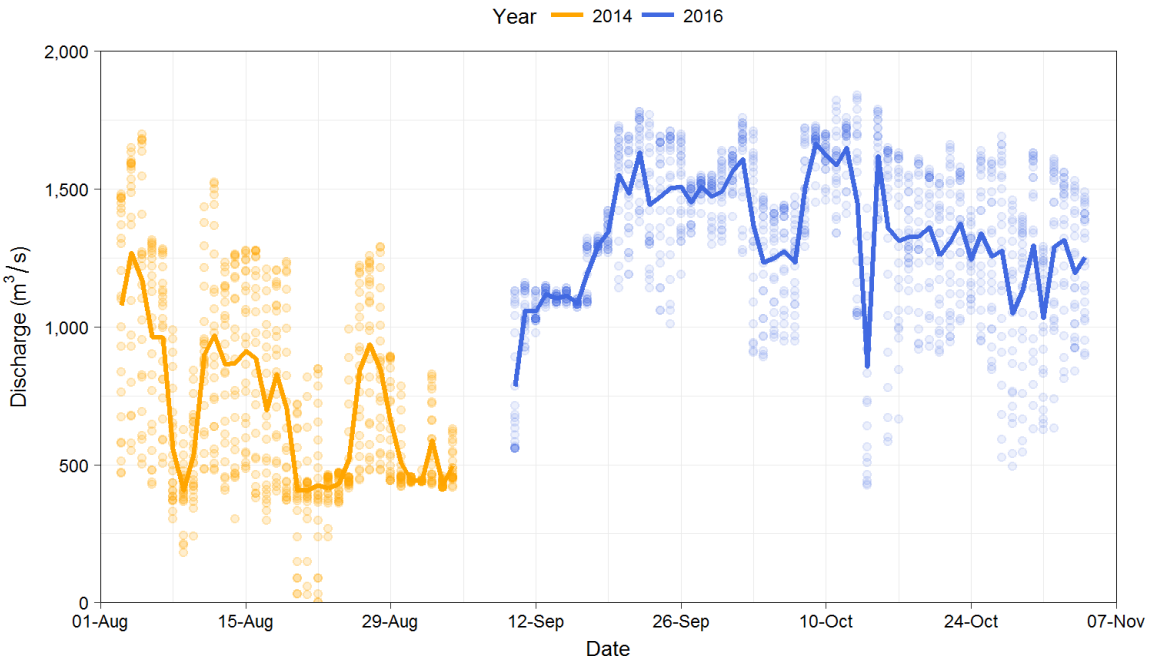

Figure 8: Hourly (points) and mean daily (lines) discharge for the Peace River above the Pine River confluence for the 2014 and 2016 periods of interest.

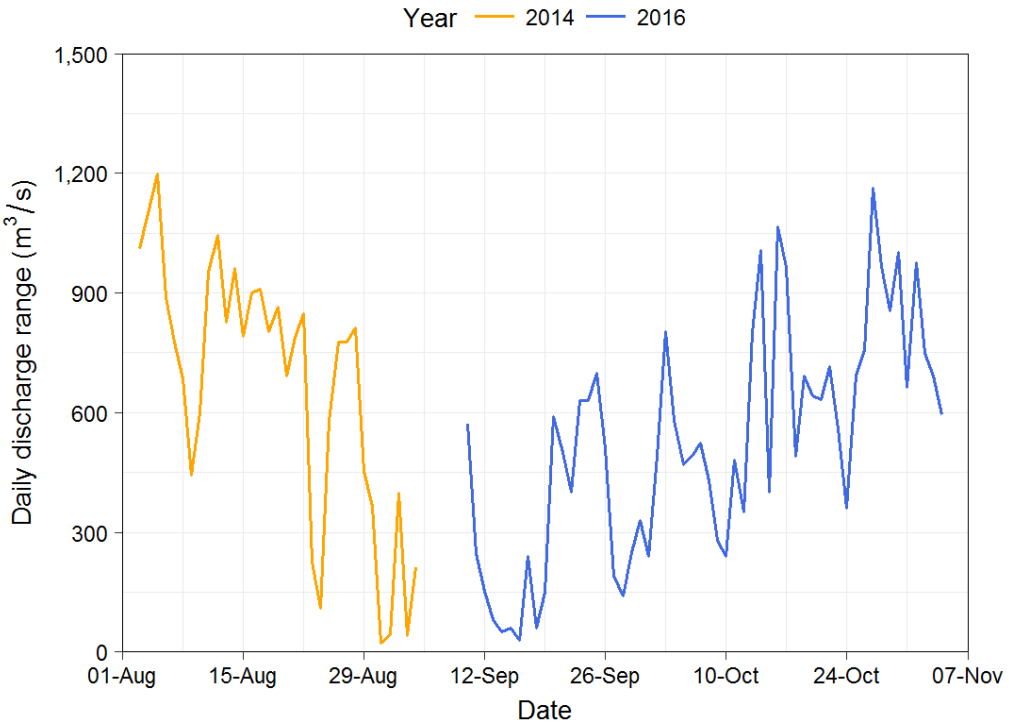

Figure 9: Daily difference between maximum and minimum hourly discharges for the Peace River above the Pine River confluence for the 2014 and 2016 periods of interest.

In 2014, mean daily water temperatures during the study period did not have a temporal trend, and varied between approximately 10ºC and 13ºC throughout August and September

(Figure 10). In comparison, in 2016, where the study period extended to early November, daily water temperatures decreased from 11-13ºC in late September to 6ºC in early November.

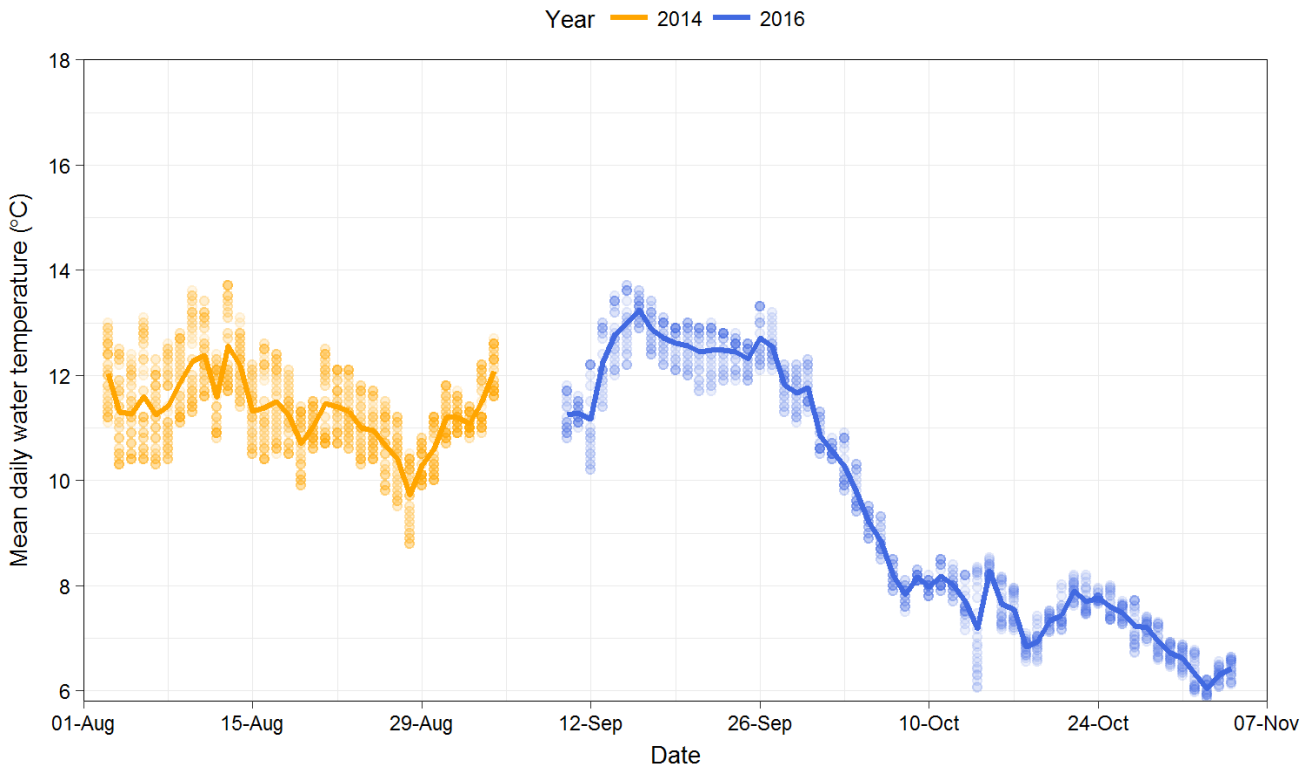

Figure 10: Hourly (points) and mean daily (lines) water temperature for the Peace River downstream of the Moberly River confluence (MobDN1) for the 2014 and 2016 periods of interest.

3.2 Fish Growth

3.2.1 Field Collections

Reliable growth data were collected from a total of 38 fish and included in the analysis – 34 age-0 Mountain Whitefish, 3 age-1 Mountain Whitefish, and 1 Longnose Sucker. The age-1 Mountain Whitefish were collected in 2014; all other fish were collected in 2016. The Longnose Sucker had a fork length of 53 mm. Age-0 Mountain Whitefish ranged in length between 76 and 116 mm FL (mean ± SD of 97 mm ± 10 mm). Age-1 Mountain Whitefish ranged in length between 170 and 175 mm FL (mean ± SD of 173 mm ± 3 mm).

3.2.2 Laboratory Analysis

The number of otolith increments counted per fish ranged from 24 to 56 for age-0 Mountain Whitefish (mean ± SD of 38.6 ± 7.3). For age-1 Mountain Whitefish, the number of otolith increments counted per fish ranged from 25 to 33 (mean ± SD of 30.0 ± 4.4). The single Longnose Sucker had 31 growth increments recorded. Fish-specific mean otolith increments ranged between 0.014 and 0.036 µm for age-0 Mountain Whitefish (mean ± SD of 0.028 ± 0.005 µm) and between 0.020 and 0.043 µm for age-1 Mountain Whitefish (mean ± SD of 0.030 ± 0.011 µm). Daily otolith increments for Longnose Sucker ranged between 0.001 and 0.022 µm (mean ± SD of 0.015 ± 0.003 µm).

3.2.3 Data Analysis

3.2.3.1 Mountain Whitefish

3.2.3.1.1 Age-0

Of the four examined candidate models, the model that included environmental variables offset by 24 h was best supported by the data (Table 1). The model's fixed effects explained 33% of the variability in otolith growth increments. The 24 h model was selected for further analysis (i.e., random effect selection and fixed effect reduction).

Table 1: Comparison of Mountain Whitefish model support for temporal offset of environmental variables using marginal Akaike's Information Criterion, corrected for small sample size.

Model	Time Offset (h)	R^2	Log-likelihood	K	mAICc	ΔmAICc[1]
1	0	0.332	4,999	22	-9,954	24
2	12	0.327	4,990	22	-9,934	43
3	24	0.338	5,011	22	-9,977	0
4	48	0.328	5,000	22	-9,955	22

Notes: R^2 describes fixed effects only (Jaegar et al 2016). K = number of estimated parameters, [1] = Difference in mAICc between the highest ranked (lowest mAICc value) model and each candidate model.

The examination of random effects indicated that a random intercept was preferred over no-random effect ($P < 0.001$). However, the addition of random slopes for the additive effects of discharge and mean water temperature (both offset by 24 h) further improved the fit of the model ($P < 0.001$). The full random effect specification therefore included fish-specific intercepts and slopes for the effects of discharge and mean water temperature. This model was used to fit the four candidate models that examined whether the effect of temperature is quadratic or linear and whether fork length is an important predictor of otolith growth in age-0 Mountain Whitefish.

Of the four multiple regression models examined, the model that included an additive effect of discharge and a quadratic effect of water temperature but did not include fish length was best supported by the data (Table 2). In this model, otolith growth increments were predicted to vary with mean daily water temperature (offset by 24 h, and expressed as a quadratic function), and with discharge range (offset by 24 h). The models' fixed effects explained 32% of the variance in otolith increments.

Table 2: Comparison of Mountain Whitefish model support for fixed effect specification using Akaike's Information Criterion, corrected for small sample size.

Model	Temperature effect	Fork length effect	R^2	Log-likelihood	K	mAICc	ΔmAICc [1]
1	Quadratic	Yes	0.338	5011	22	-9977	5
2	Linear	Yes	0.314	4997	19	-9955	28
3	Quadratic	No	0.323	5010	18	-9983	0
4	Linear	No	0.319	4995	16	-9958	25

Notes: R^2 describes fixed effects only (Jaegar et al 2016). K = number of estimated parameters, [1] = Difference in mAICc between the highest ranked (lowest mAICc value) model and each candidate model.

Mean daily otolith growth (when environmental variables were at their average values) was estimated to be 0.03 µm. The effects of the interaction between discharge and water temperature were not significant (P>0.05; Figure 11), indicating an additive, rather than multiplicative, effect of the two variables on otolith growth. Both main effects (discharge range and the quadratic function of mean daily temperature) were significantly different from zero (P=0.001, P<0.001, and P<0.001, respectively). The estimated effect size of 1 SD change in temperature on otolith growth was larger than that of 1 SD change in discharge range, given the range of observed values for both variables (Figure 11). However, due to the second degree polynomial, the specific effect depended on the values of the two variables. An increase of 1 SD (1.9ºC) in mean water temperature from its average value (8.4ºC) resulted in a predicted increase of 0.003 µm when discharge range was held at average value (612 m³/s). In comparison, an increase of 2 SD in water temperature resulted in an increase of only 0.001 µm. That is, when discharge was average, an increase of 1 SD and 2 SD in temperature resulted in a 10% and 2% increase in otolith growth, respectively. Conversely, an increase of 1 SD (90.8 m³/s) in discharge range when water temperature was at its average value (8.4ºC) resulted in a decrease of 0.001 µm. When discharge range increased by 1 SD (264 m³/s) from its average value of 612 m³/s, predicted otolith growth decreased by 0.001 µm when temperature was held at average value.

Predicted daily otolith growth increments decreased with discharge range, whereas increase in temperature was predicted to increase otolith increments at low temperatures (6-10ºC) and reduce otolith increments at temperatures of 11-12ºC (Figure 12). For example, when discharge range was at average, a 2ºC increase from 6ºC to 8ºC increased the size of the daily predicted otolith increment by 0.009 µm, whereas a 2ºC increase from 10ºC to 12ºC decreased the size of the daily predicted otolith increment by 0.002 µm. The different magnitudes and directions of the effect of temperature on otolith growth increment reflect the second-degree polynomial function of temperature in the model selected for interpretation.

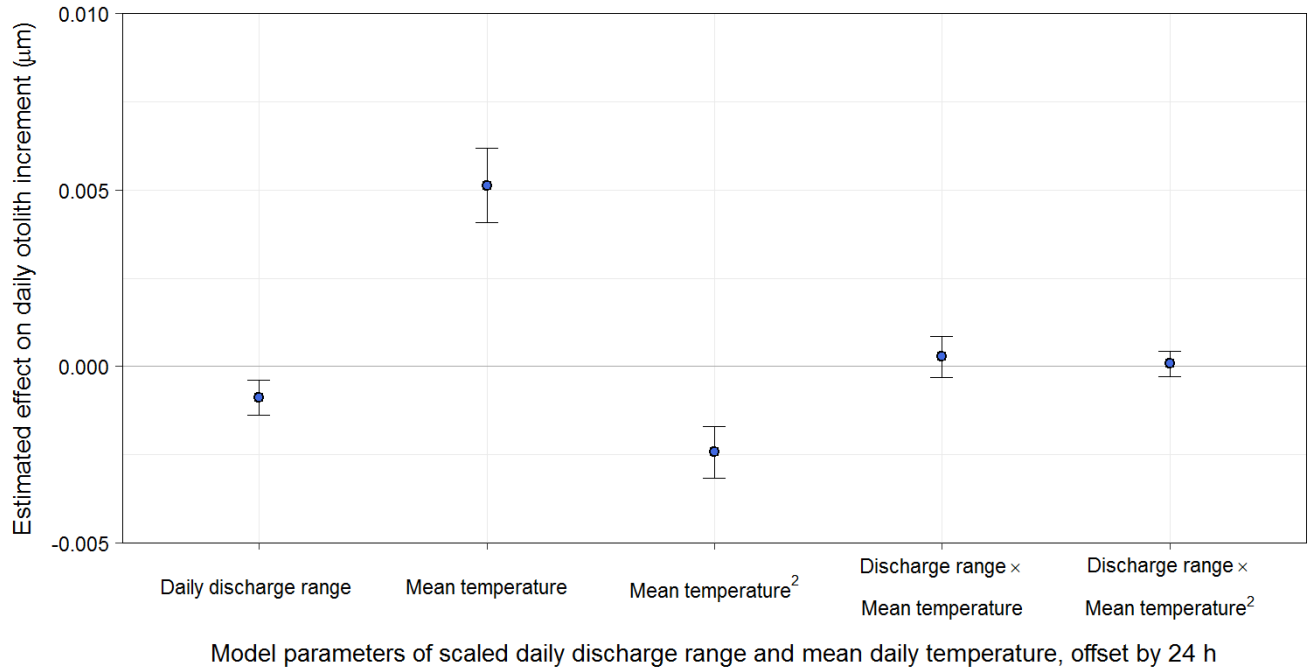

Figure 11: Estimated age-0 Mountain Whitefish model effects. The effects describe the change in otolith growth with an increase of 1 SD in the value of the respective environmental variable. Error bars are 95% confidence intervals.

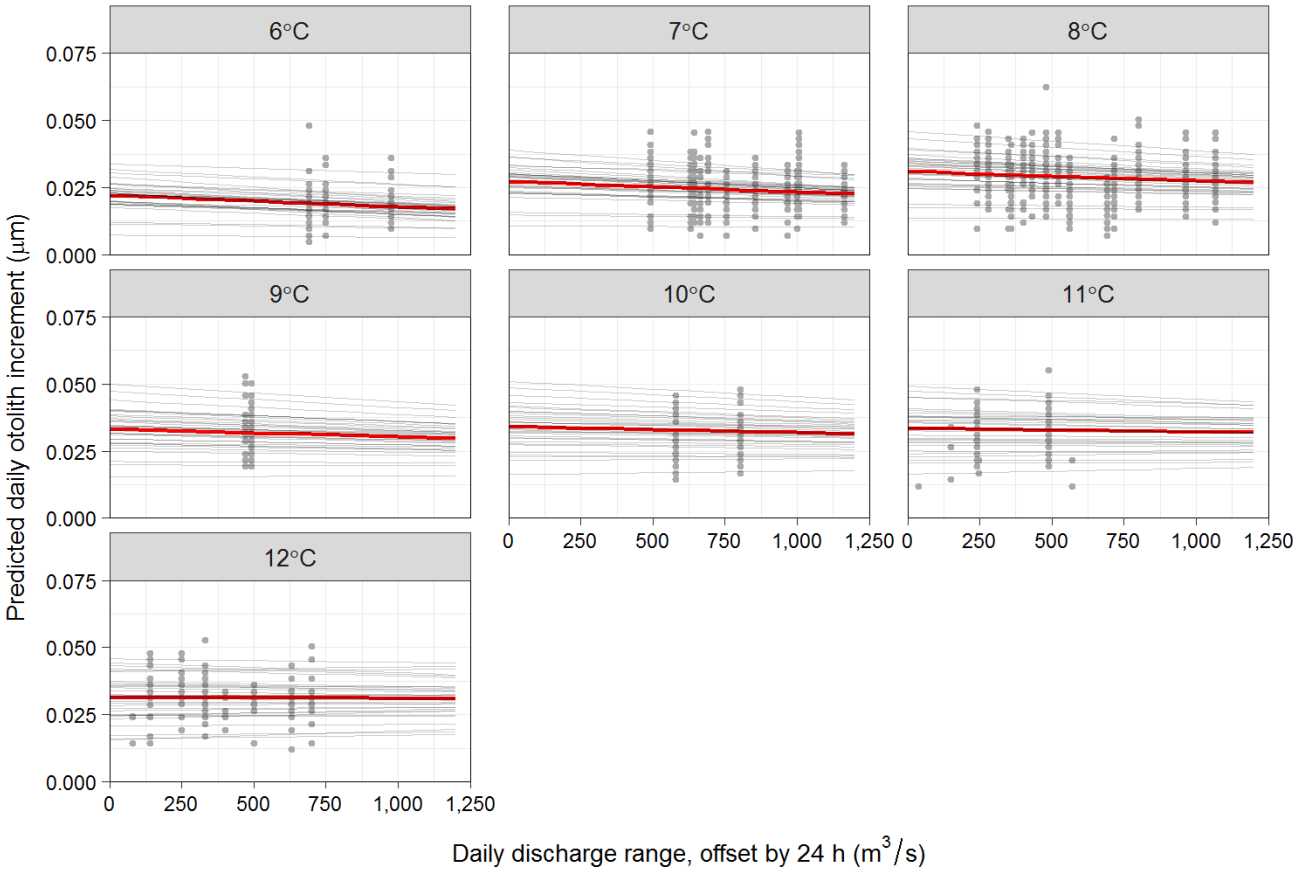

Figure 12: Predicted Mountain Whitefish otolith growth increments as a function of mean daily water temperature (offset by 24 h) and daily discharge range (offset by 24 h). Raw data are shown as points, fish-specific predictions are shown in light grey, and mean (population-level) response is shown in red in each panel.

Overall, the selected model predicted otolith growth well, while accounting for individual variability between age-0 Mountain Whitefish specimens (Figure 13), although the fixed effects explained only 32% of the variance in otolith growth data (Table 2). The inclusion of water temperature as a predictor in the model accounted for much of the variability in otolith increment data, evident in a wide spread of otolith increment values at the same discharge range.

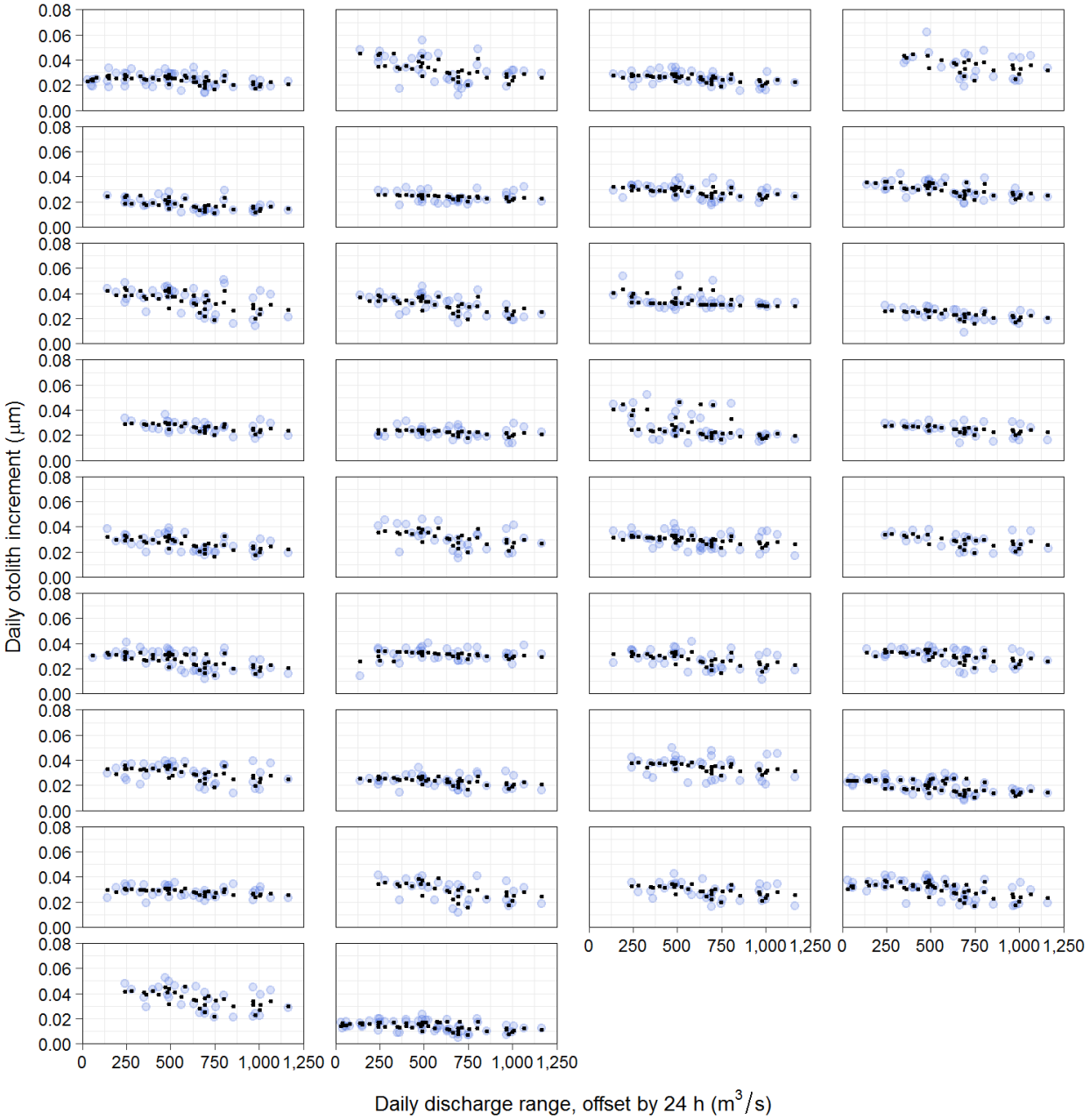

Figure 13: Age-0 Mountain Whitefish raw otolith increment data, plotted against daily discharge range, offset by 24 h. Blue points are raw data, and the overlaid black points are fish-specific model predictions. Each panel represents an individual fish.

The mAICc support for a quadratic function of day of study as a predictor was high (mAICc value of -10,314, compare to values in Table 1). Although predictions from the day-only model were estimated (Figure 14), the model's assumptions of linearity and residual normality were not met (data not shown), indicating that day did not capture the overall pattern of data. This means that the model's prediction may be biased and that the significance of the model's parameters may be inaccurate.

Day of study is used here as a rough, and likely inaccurate, estimate of age, since Mountain Whitefish hatch can occur over an extended period. Since discharge range was highly correlated with time (Figure 9), the inclusion of day in the models of otolith increments along with temperature and discharge is likely to distort results due to confounding. If future samples focus on younger fish, where age (in days) could be determined, the addition of age effects to models that include environmental variables (discharge and temperature) may improve model fit and explain variability in the observed otolith increment data.

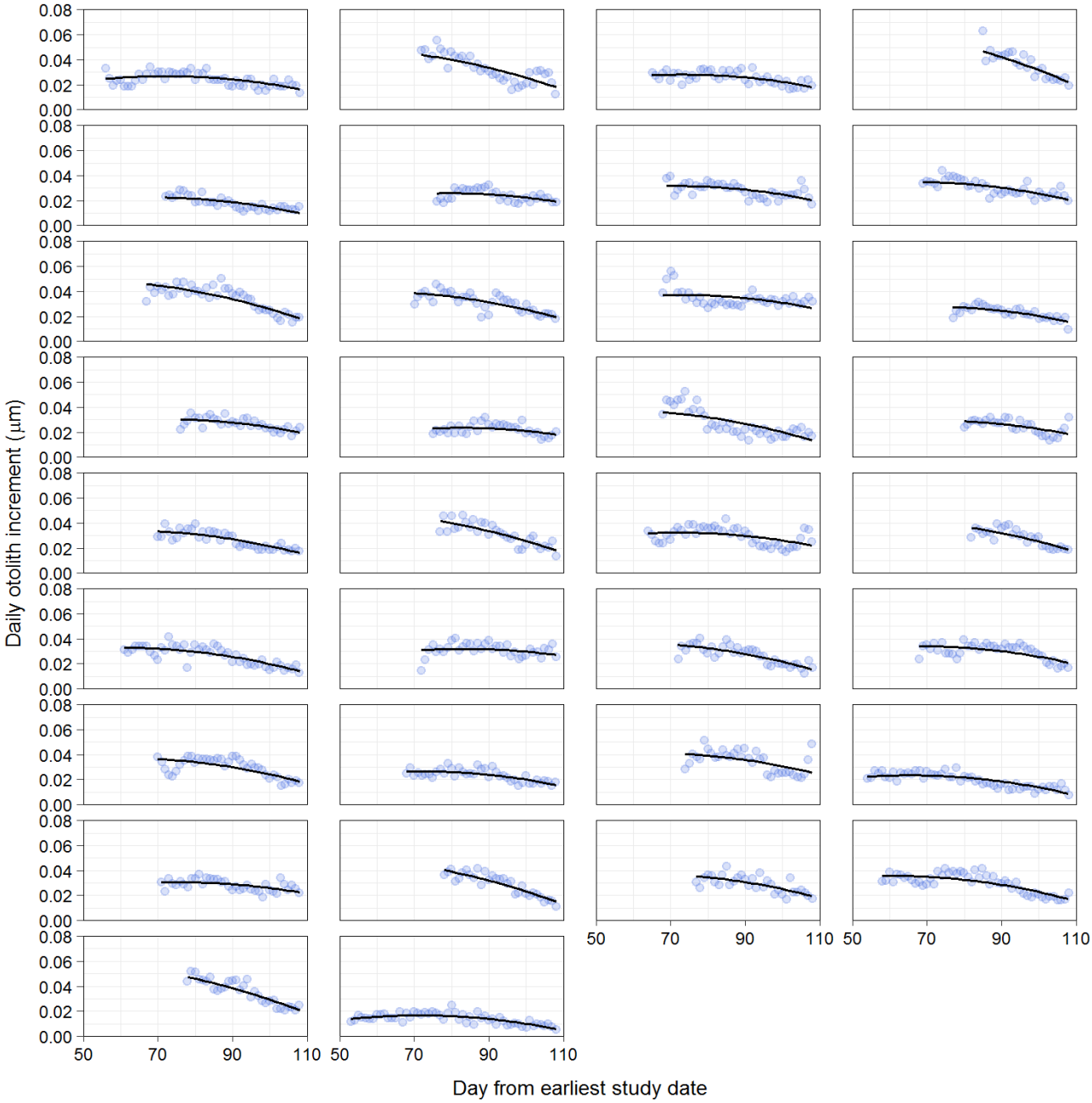

Figure 14: Age-0 Mountain Whitefish raw otolith increment data, plotted against day of study; lines represent fish-specific model predictions.

3.2.3.1.2 Age-1

Of the four examined candidate models, the models that included environmental variables without an offset or with an offset by 24 h were best supported by the data (Table 3). To retain comparability with age-0 Mountain Whitefish analysis, the model with 24 h offset was selected for further analysis. The model's fixed effects explained 12% of the variance in otolith growth increments. Fork length was not included as an independent variable, due to the limited sample size.

Table 3: Comparison of age-1 Mountain Whitefish model support for temporal offset of environmental variables using marginal Akaike's Information Criterion, corrected for small sample size.

Model	Time Offset (h)	R^2	Log-likelihood	K	mAICc	ΔmAICc[1]
1	0	0.119	341	6	-670	0
2	12	0.095	340	6	-667	3
3	24	0.115	341	6	-669	1
4	48	0.092	340	6	-667	3

Notes: R^2 describes fixed effects only (Jaegar et al 2016). K = number of estimated parameters, [1] = Difference in mAICc between the highest ranked (lowest mAICc value) model and each candidate model.

The examination of random effects indicated that a random intercept was preferred over no-random effect ($P < 0.001$). However, the addition of random slopes for the additive effects of discharge and mean water temperature (both offset by 24 h) did not improved further the fit of the model ($P = 0.07$). Therefore, only random fish-specific intercepts were used in the analysis.

Of the two multiple regression models examined (which assessed whether temperature effect was linear or quadratic), the model that included a linear effect of temperature had better support (Table 4). In this model, otolith growth increments of age-1 Mountain Whitefish were predicted to vary with mean daily water temperature (offset by 24 h, and expressed as a linear function), and with discharge range (offset by 24 h). The model's fixed effects explained only 11% of the variance in otolith increments.

Table 4: Comparison of age-1 Mountain Whitefish model support for multiple regressions using Akaike's Information Criterion, corrected for small sample size.

Model	Temperature effect	R^2	Log-likelihood	K	mAICc	ΔmAICc[1]
1	Quadratic	0.115	341.2	7	-670	2
2	Linear	0.113	341.1	6	-672	0

Notes: R^2 describes fixed effects only (Jaegar et al 2016). K = number of estimated parameters, [1] = Difference in mAICc between the highest ranked (lowest mAICc value) model and each candidate model.

Mean daily otolith growth (when environmental variables were at their average values) was estimated to be 0.03 µm. The effect of water temperature on otolith growth was not significant (*P* = 0.07, Figure 15), while the effect of discharge was significantly different from zero (*P* = 0.001). An increase of 1 SD (297 m³/s) in discharge range from its average value (721 m³/s) resulted in a predicted increase of 0.001 µm in otolith growth when water temperature was held at average value (11.4ºC).

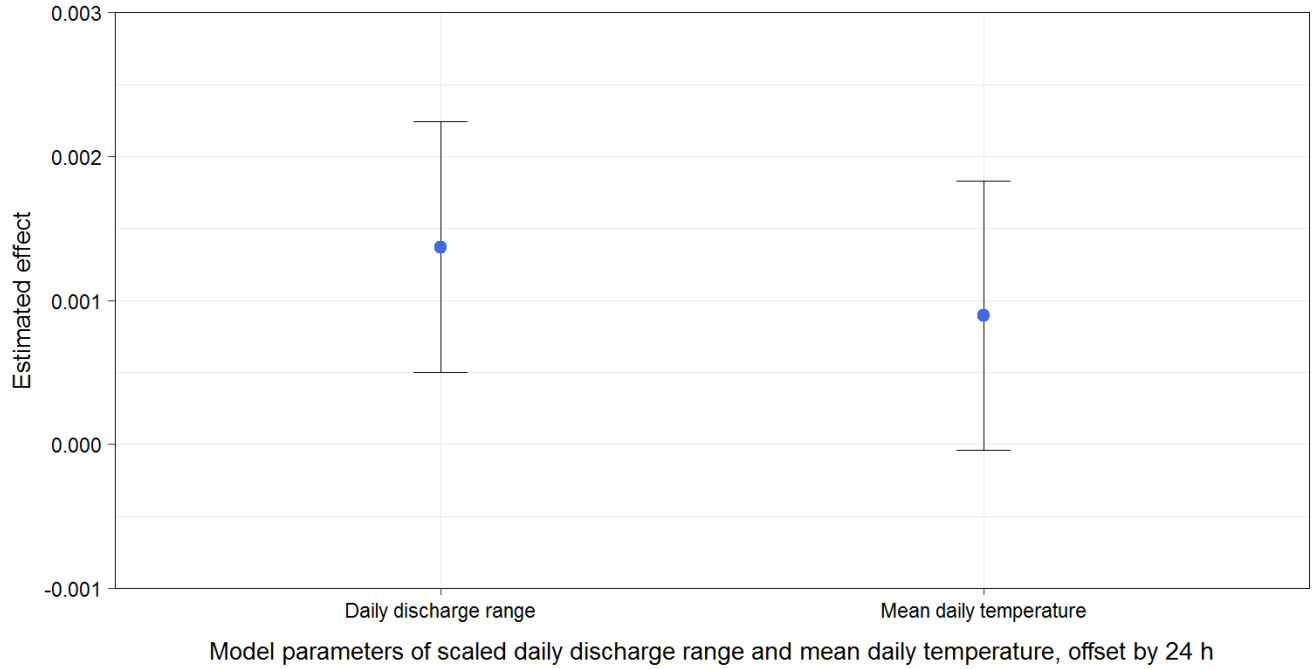

Figure 15: Estimated age-1 Mountain Whitefish model effects. The effects describe the change in otolith growth with an increase of 1 SD in the value of the respective environmental variable. Error bars are 95% confidence intervals.

Predicted daily otolith growth increments increased by 0.0005 µm with every 100 m³ increase in discharge range (Figure 16). For example, at 9ºC, predicted growth increment at the highest discharge range (1,200 m³/s) was 24% larger than under no discharge fluctuation (0 m³/s). Overall, the selected model predicted increased otolith growth with increases in either discharge range or mean water temperature (the latter effect not significantly different from zero). However, the fixed effects only accounted for 11% of the variance in otolith increment growth. The low proportion of explained variability and the very small sample size necessitate very cautious interpretation of the presented results.

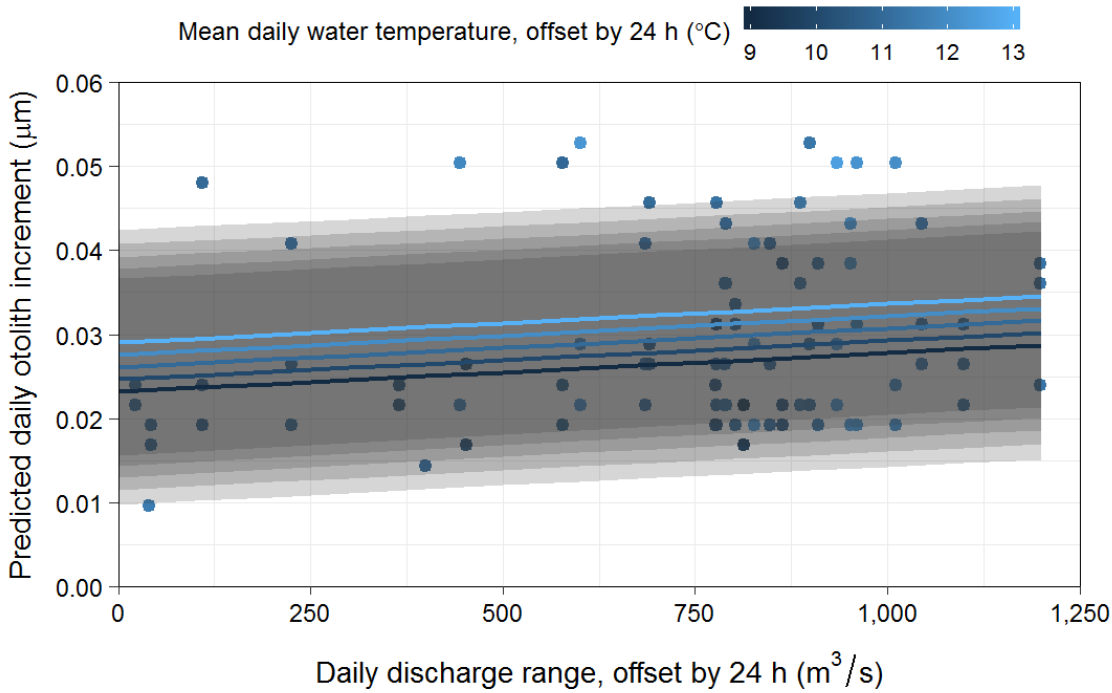

Figure 16: Predicted age-1 Mountain Whitefish otolith growth increments as a function of daily discharge range (without offset). Separate prediction lines were drawn for scenarios of 6ºC, 7ºC, 8ºC, and 9ºC; grey ribbons are 95% confidence bands.

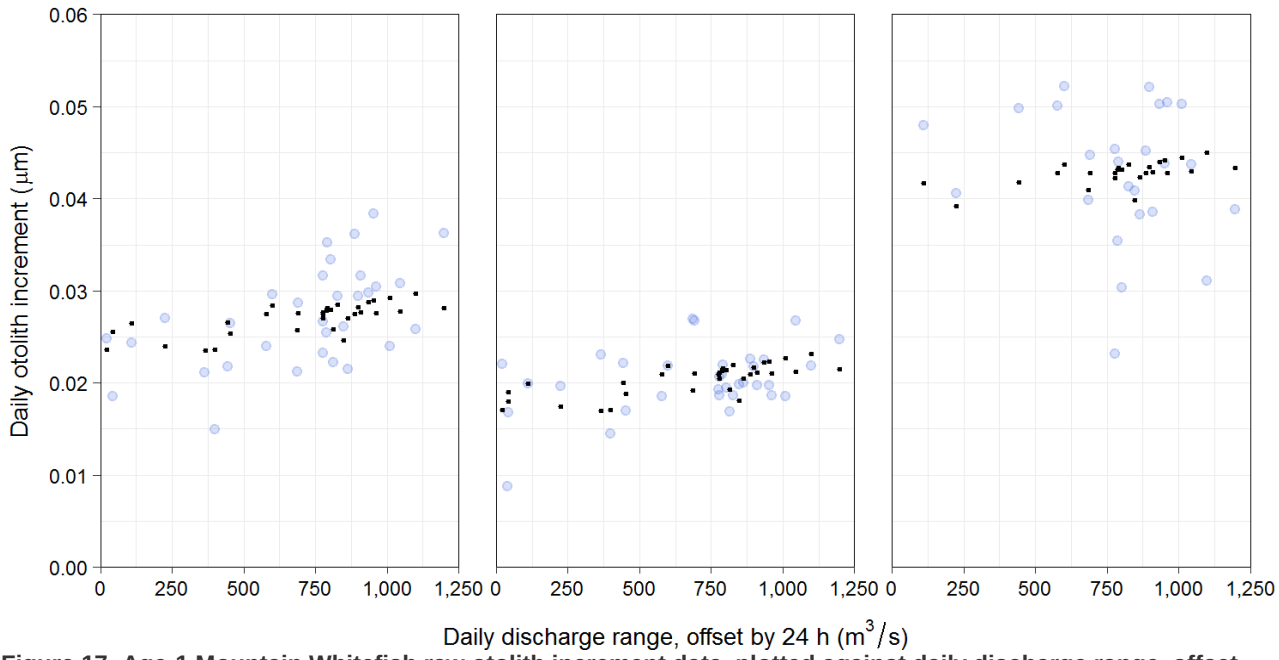

Figure 17: Age-1 Mountain Whitefish raw otolith increment data, plotted against daily discharge range, offset by 24 h. The overlaid black points are fish-specific model predictions. Each panel represents an individual fish.

3.2.3.2 Longnose Sucker

The results of Longnose Sucker otolith growth analysis should be interpreted with caution because the dataset consisted of a single fish; individual variability could not be assessed.

Moreover, since the data rely on a single year's collection of discharge and temperature, any correlation between the two variables, which would be reduced by inclusion of multiple years of data, would strongly influence the current results. The two models with 12 h offsets had the best support of the eight candidate models (Table 5). The linear and quadratic versions of the 12 h offset data had similar support (ΔAICc of 1), therefore the simpler, linear model was selected, even though its R^2 value was somewhat lower. In this model, otolith growth increments were predicted to vary with mean daily water temperature (offset by 12 h, and expressed as a linear function), and with discharge range (offset by 12 h). The environmental variables explained 51% of the variance in otolith growth. Fork length was not included in the models because the dataset consisted of a single fish.

Table 5: Comparison of Longnose Sucker model support for environmental variables and temporal offset using Akaike's Information Criterion, corrected for small sample size

Model	Time Offset (h)	Temperature effect	R^2	Log-likelihood	K	AICc	ΔAICc[1]
1	0	Quadratic	0.442	144	5	-275	8
2	0	Linear	0.391	142	4	-275	8
3	12	Quadratic	0.570	148	5	-283	0
4	12	Linear	0.512	146	4	-282	1
5	24	Quadratic	0.499	145	5	-278	5
6	24	Linear	0.445	144	4	-278	5
7	48	Quadratic	0.411	143	5	-274	10
8	48	Linear	0.395	143	4	-276	8

Notes: R^2 describes fixed effects only (Jaegar et al 2016). K = number of estimated parameters, [1] = Difference in AICc between the highest ranked (lowest AICc value) model and each candidate model.

Mean daily otolith growth (when environmental variables were at their average values) was estimated to be 0.014 µm. Both environmental effects were significantly different from zero (P=0.02 for discharge range and P<0.001 for mean daily temperature; Figure 18). The effect of temperature was larger than that of discharge – with 1 SD change in mean daily water temperature (0.8ºC) from the mean temperature (7.5ºC), otolith increments were estimated to increase by 0.0017 µm (11% of intercept value). On the other hand, with 1 SD increase in daily discharge range (281 m³/s) from the average range (674 m³/s), otolith increments were predicted to decrease by 0.001 µm (7% of intercept value).

The model predicted a decrease in otolith increments as a function of discharge range, offset by 12 h (Figure 19). For every increase of 100 m³/s in discharge range (offset by 12 h), daily otolith growth decreased by 0.004 µm. For example, at 7ºC, predicted growth increment at the highest discharge range (1,500 m³/s) was 34% smaller than under no discharge fluctuation (0 m³/s). The effect of mean water temperature resulted in an increase of 0.002 µm in predicted otolith increment growth with every 1ºC increase in water temperature. This increase, when expressed as percentage increase, ranged between 10% and 24%, depending on discharge range.

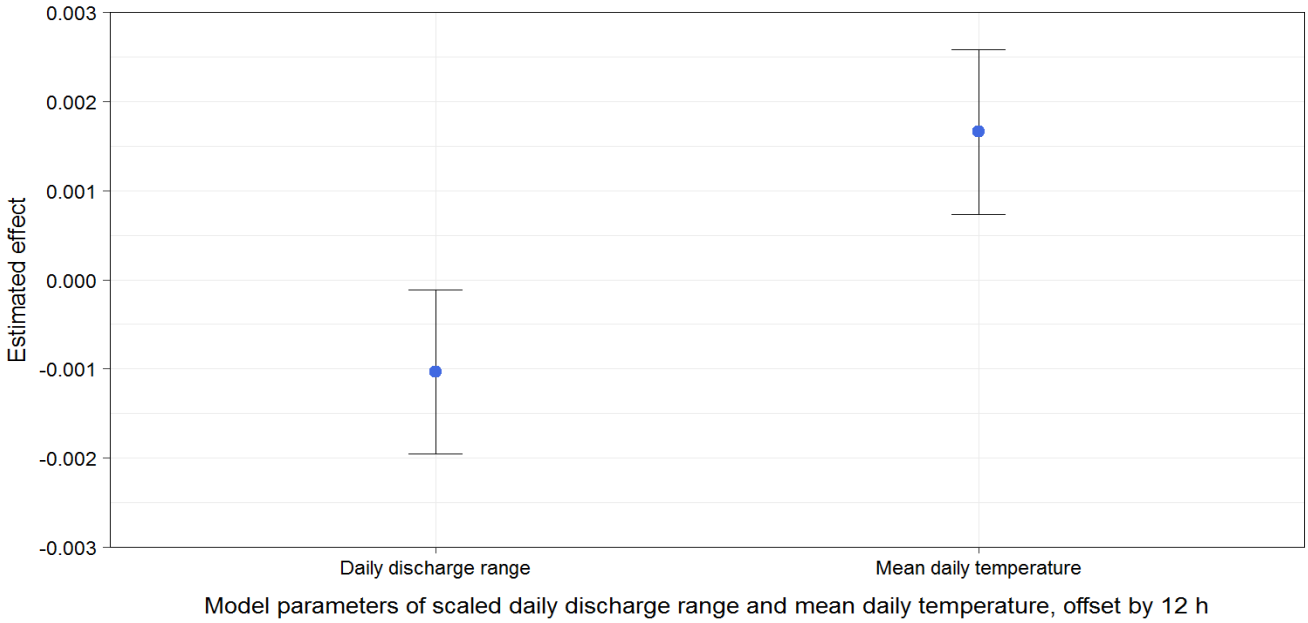

Figure 18: Estimated Longnose Sucker model effects. The effects describe the change in otolith growth with an increase of 1 SD in the value of the respective environmental variable. Error bars are 95% confidence intervals.

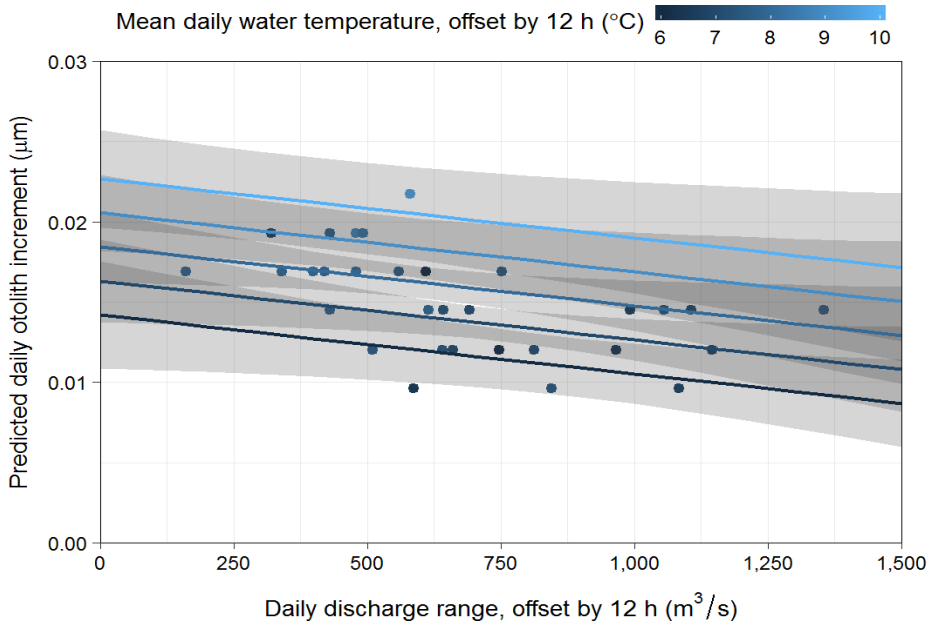

Figure 19: Predicted Longnose Sucker otolith growth increments as a function of mean daily water temperature (offset by 12 h) and daily discharge range (offset by 12 h). Separate prediction lines were drawn for scenarios of 6ºC, 7ºC, 8ºC, and 9ºC; grey ribbons are 95% confidence bands.

Overall, the selected model predicted otolith increments well (Figure 20). The inclusion of water temperature as a predictor in the model accounted for much of the variability in otolith increment data (e.g., both high and low values of otolith increments at a discharge range of approximately 550 m³/s).

The AICc support for day of study as a predictor was not high (AICc value of -279, compare to values in Table 5). The model predicted a reduction in otolith growth rate with time (Figure 21). As opposed to the Mountain Whitefish model of day-only influence, modeling assumptions of

linearity and normality were met for Longnose Sucker. However, since the model is based on a single fish, the variability of otolith growth rate is likely strongly underestimated. In addition, since both temperature (Figure 10) and discharge range (Figure 9) had strong temporal trends in 2016, the day-only model likely confounds effects of age, temperature, and discharge variability. This model is only presented as an alternative to the models above, which assumed a constant growth rate as a function of age.

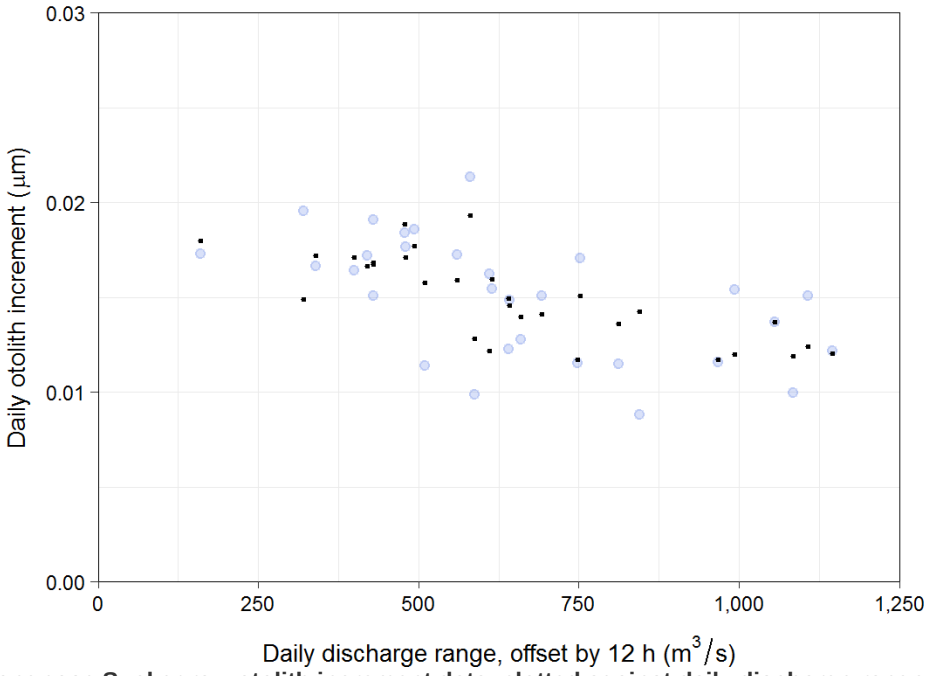

Figure 20: Longnose Sucker raw otolith increment data, plotted against daily discharge range, offset by 12 h. The overlaid black points are model-predicted values.

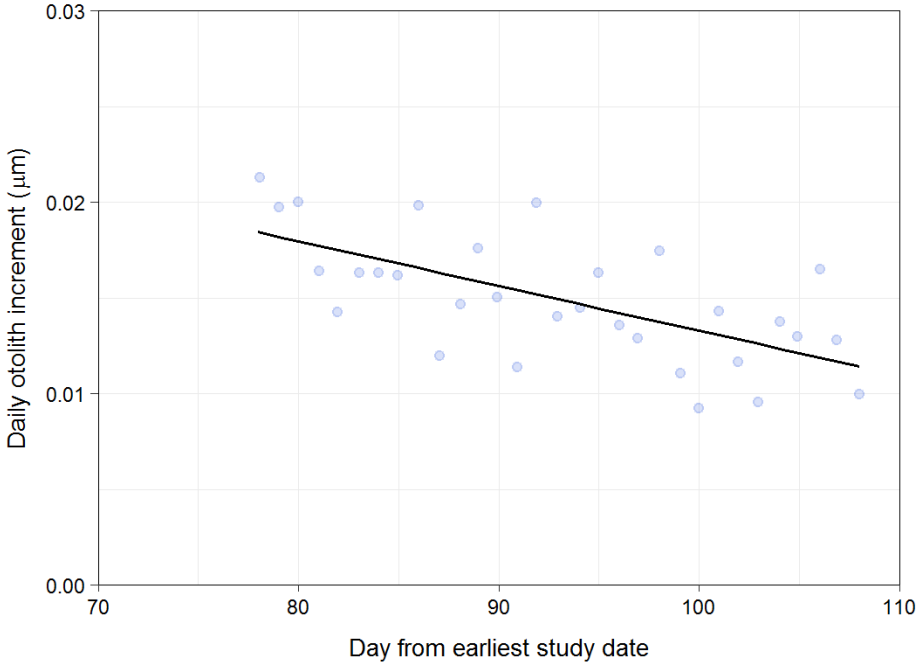

Figure 21: Longnose Sucker raw otolith increment data, plotted against day of study; line represents model predictions.

4.0 CONCLUSIONS

Overall, the models predicted otolith growth patterns well across years, species, and individual fish. The fixed effects (discharge range and water temperature) explained 30-40% of the variance in otolith growth in age-0 Mountain Whitefish and in Longnose Sucker. However, individual variability was only accounted for in the Mountain Whitefish analysis because only a single Longnose Sucker was available for analysis. In addition, the sample size of age-1 Mountain Whitefish was very small, and the fixed effects explained only 11% of the variance in otolith growth of age-1 Mountain Whitefish, suggesting that the results of age-1 Mountain Whitefish analysis should be interpreted with caution.

4.1 Management Hypothesis

The examined models suggest that an increase in daily discharge range influences otolith growth in both Mountain Whitefish and Longnose Sucker. In Mountain Whitefish, the relationship differed between age-0 and age-1 fish. For age-0 fish, an increase of discharge range resulted in a decrease in otolith growth increments, whereas for age-1 fish, an increase of discharge range resulted in an increase in otolith growth increments. However, the age-1 dataset had a limited sample size (n = 3), and both datasets only constituted a single year of data. Increased sample sizes and the addition of variable discharge and temperature scenarios (collected across multiple years) may reduce confounding, improve model fit, and provide clearer and more accurate predictions of the effect of environmental variables on otolith growth rates. For Longnose Sucker, increased discharge range resulted in decreased otolith growth rate, although growth strongly depended on temperature. The Longnose Sucker model was based on a single fish and the results should therefore be interpreted with caution; individual variability could not be assessed.

4.2 Limitations of Analysis

The results of models of otolith growth as a function of day of study suggested that age may be an important predictor of otolith growth rate in age-0 Mountain Whitefish and Longnose Sucker during the period of interest. In this work, day of study was used as a rough substitution of fish age, since it was not possible to determine the ages of the captured fish.

Individual variability of otolith growth in Longnose Sucker was not accounted for, since only a single specimen was included in the analysis.

Due to limited sample size, the variability of age-1 Mountain Whitefish was likely underestimated, despite being included in the model specification.

The inclusion of a single year of data for each of the examined datasets (age-0 Mountain Whitefish, age-1 Mountain Whitefish, and Longnose Sucker) increased the likelihood of confounding environmental effects. For example, the 2016 discharge range increased over time, while the mean daily temperature decreased over time. This resulted in a negative relationship between discharge range and water temperature, that may have affected model selection and model estimates.

4.3 Future Work

The collection of young fish, whose ages could be determined based on the count of daily otolith increments, may allow the addition of age to the models that include the effects of environmental variables. This would allow accounting for the variability in otolith increment deposition due to age, which would improve model fit and interpretation.

Much of the variability associated with otolith increment data was not accounted for by the constructed models. It may be of interest to perform an analysis of measurement error to estimate the extent of influence of measurement error on otolith growth rate variability.

5.0 CLOSURE

We trust this information is sufficient for your needs at this time. Should you have any questions or concerns, please do not hesitate to contact the undersigned.

GOLDER ASSOCIATES LTD.

Dustin Ford, BSc, RPBio
Project Manager, Fisheries Biologist

Shawn Redden, RPBio
Associate, Senior Fisheries Biologist

6.0 REFERENCES

Aldanondo. N., Cotano U., Tiepolo M., Boyra G., and Irigoien X. 2010. Growth and movement patterns of early juvenile European anchovy (Engraulis encrasicolus L.) in the Bay of Biscay based on otolith microstructure and chemistry. Fisheries Oceanography 19 (3): 196-208.

BC Hydro. 2016. Site C Clean Energy Project - Peace River Water Level Fluctuation Monitoring Program. 10 pp.

Cotano U., Alvarez P. 2003. Growth of young-of-the-year mackerel in the Bay of Biscay. Journal of Fish Biology 62(5):1010 – 10.

Golder Associates Ltd. and W.J. Gazey Research. 2015. GMSMON-2 Peace Project Water Use Plan – Peace River Fish Index – 2014 Investigations. Report prepared for BC Hydro, Burnaby, British Columbia. Golder Report No. 1400753. 68 pages + 6 appendices.

Jaeger B.C., Edwards L.J., Das K. and Sen P.K. 2016: An R^2 statistic for fixed effects in the generalized linear mixed model, Journal of Applied Statistics

R Core Team (2017). R: A language and environment for statistical computing. R Foundation for Statistical Computing, Vienna, Austria. URL https://www.R-project.org/.

Schneidervin, R.W, W.A. Hubert. 1986. A Rapid Technique for Otolith Removal from Salmonids and Catostomids. N. Am. Fish Manage 6(2): 287.

Vaida F. and Blanchard S. 2005. Conditional Akaike Information for mixed-effects models. Biometrika 92(2): 351-370.

Zuur A, Leno EN, Walker N, Saveliev AA, Smith GM. 2009. Mixed effects models and extensions in ecology with R. Springer, 574 s.